FINNISH METEOROLOGICAL INSTITUTE
CONTRIBUTIONS

NO. 62

OBSERVATIONS OF PRODUCTION AND TRANSPORT OF NO_x FORMED BY ENERGETIC PARTICLE PRECIPITATION IN THE POLAR NIGHT ATMOSPHERE

ANNIKA SEPPÄLÄ

DEPARTMENT OF PHYSICAL SCIENCES
FACULTY OF SCIENCE
UNIVERSITY OF HELSINKI
HELSINKI, FINLAND

ACADEMIC DISSERTATION in physics

To be presented, with the permission of the Faculty of Science of the University of Helsinki, for public critisism in Auditorium D 101 at Physicum in Kumpula Campus (Gustaf Hällströmin katu 2b) on September 28th, 2007, at 12 o'clock noon.

Finnish Meteorological Institute
Helsinki, 2007

ISBN 978-951-697-627-6 (paperback)
ISBN 978-952-10-4181-5 (PDF)
ISSN 0782-6117

Yliopistopaino
Helsinki, 2007

FINNISH METEOROLOGICAL INSTITUTE

Published by Finnish Meteorological Institute
(Erik Palménin aukio 1) P.O. Box 503
FI-00101 Helsinki, Finland

Series title, number and report code of publication
Contributions 62, FMI-CONT-62

Date
September 2007

Authors
Annika Seppälä

Name of project

Commissioned by

Title

Observations of production and transport of NO_x formed by energetic particle precipitation in the polar night atmosphere

Abstract

This work is focused on the effects of energetic particle precipitation of solar or magnetospheric origin on the polar middle atmosphere. Most of these energetic particles are protons and electrons with MeV and keV energies, respectively. The energetic charged particles have access to the atmosphere in the polar areas, where they are guided by the Earth's magnetic field. In the polar areas the energetic particles penetrate down to 20-100 km altitudes (stratosphere and mesosphere) ionising the ambient air. This ionisation leads to production of odd nitrogen (NO_x) and odd hydrogen (HO_x) species, which take part in catalytic ozone destruction. NO_x has a very long chemical lifetime during polar night conditions. Therefore NO_x produced at high altitudes during polar night can be transported to lower stratospheric altitudes, where it contributes to the ozone balance.

Particular emphasis in this thesis is in the use of both space and ground based observations: ozone and nitrogen dioxide (NO_2) measurements from the GOMOS instrument on board the European Space Agency's environmental satellite Envisat are used together with subionospheric VLF radio wave observations from ground stations. Combining the two observation techniques enabled detection of NO_x enhancements throughout the middle atmosphere, including tracking the descent of NO_x enhancements of high altitude origin down to the stratosphere.

GOMOS observations were used to examine the effect of the large Solar Proton Events of October-November 2003 on the Northern Hemisphere polar middle atmosphere. The results showed the progression of the SPE initiated NO_x enhancements through the polar winter. In the upper stratosphere nighttime NO_2 increased by an order of magnitude, and the effect was observed to last for several weeks after the SPEs. Ozone decreases up to 60 % from the pre-SPE values were observed in the upper stratosphere nearly a month after the events. Over several weeks the GOMOS observations showed the gradual descent of the NO_x enhancements to lower altitudes. GOMOS measurements from years 2002-2006 were used to study polar winter NO_x increases and their connection to energetic particle precipitation. NO_x enhancements were found to occur in a good correlation with both increased high-energy particle precipitation and increased geomagnetic activity. The average wintertime polar NO_x was found to have a nearly linear relationship with the average wintertime geomagnetic activity.

The results from this thesis work show how important energetic particle precipitation from outside the atmosphere is as a source of odd nitrogen in the middle atmosphere, and thus its importance to the chemical balance of the atmosphere.

Publishing unit
Earth Observation

Classification (UDC)
551.501, 551.590.2

Keywords
stratosphere, mesosphere, odd nitrogen, ozone, energetic particle precipitation, solar storms

ISSN and series title
0782-6117 Finnish Meteorological Institute Contributions

ISBN
978-951-697-627-6 (paperback), 978-952-10-4181-5 (PDF)

Language
English

Sold by
Finnish Meteorological Institute / Library
P.O. Box 503, FI-00101 Helsinki Note
Finland

Pages
100

Price

ILMATIETEEN LAITOS

Julkaisija: Ilmatieteen laitos, (Erik Palménin aukio 1)
PL 503, 00101 Helsinki

Julkaisun sarja, numero ja raporttikoodi
Contributions 62, FMI-CONT-62
Julkaisuaika
Syyskuu 2007

Tekijä(t)
Annika Seppälä

Projektin nimi

Toimeksiantaja

Nimeke
Havaintoja korkeaenergisen hiukkaspresipitaation ilmakehässä tuottamista typen oksideista ja niiden kulkeutumisesta polaariyössä

Tiivistelmä

Tässä väitöskirjatyössä on tutkittu maan napa-alueiden ilmakehään auringosta tai maan magnetosfääristä tulevien korkeaenergisten varattujen hiukkasten vaikutuksia ilmakehän koostumukseen. Nämä korkeaenergiset hiukkaset, joista pääosa on elektroneita ja protoneita, tunkeutuvat maan napa-alueiden ilmakehään ionisoiden sitä noin 20 ja 100 kilometrin välisellä korkeusalueella. Tämä korkeusalue kattaa stratosfääri- ja mesosfääri-kerrokset ja sitä kutsutaan yleisesti keski-ilmakehäksi. Keski-ilmakehässä varattujen hiukkasten aiheuttamasta ionisaatiosta seuraa typen ja vedyn oksidien tuottoa. Sekä typen että vedyn oksidit aiheuttavat ilmakehässä otsonikatoa katalyyttisten kemiallisten reaktioketjujen välityksellä. Typen oksidit (NO_x) ovat ilmakehässä napa-alueiden valottomina aikoina hyvin pitkäikäisiä, voiden siten vaikuttaa ilmakehän otsonitasapainoon pitkinä talvisina ajanjaksoina.

Työssä on käytetty erityisesti Euroopan avaruusjärjestön Envisat-ympäristösatelliitissa olevan suomalais-ranskalaisen GOMOS-mittalaitteen havaintoja ilmakehän yöaikaisesta koostumuksesta. Toisin kuin ilmakehän koostumusta tutkivat mittalaitteet yleensä, GOMOS kykenee tekemään havaintoja öisestä ilmakehästä käyttämällä mittauksissa apuna tähdistä tulevaa säteilyä. GOMOS-mittalaitteen avulla havaittiin ensimmäistä kertaa kuinka Auringossa loka-marraskuussa 2003 tapahtuneiden myrskyjen seuraksena pohjoisen napa-alueen ilmakehän typen oksidien pitoisuus kasvoi ja kuinka kasvaneet pitoisuudet säilyivät ilmakehässä napa-alueen talven aikana saaden aikaan otsonikatoa ylästratosfäärissä ja mesosfäärissä.

GOMOS-mittalaitteen havaintojen avulla todettiin myös, että talvisten napa-alueiden ilmakehän keskimääräisen typen oksidien määrän ja ilmakehään pääsevien korkeaenergisten hiukkasten välillä on yhteys myös muulloin kuin aktiivisina aurinkomyrskyaikoina. Tämä yhteys oli aiemmin havaittu eteläisellä napa-alueella, mutta GOMOSin uudet yöaikaiset havainnot ilmakehästä paljastivat saman ilmiön myös pohjoisella napa-alueella.

Yhdistämällä GOMOS-mittalaitteen havainnot radioaallonpituuksilla tehtävien niin kutsuttujen VLF eli Very Low Frequency mittausten kanssa, saatiin täysin uutta tietoa ilmakehän koostumuksesta. Väitöskirjatyöhön liittyen kehitettiin menetelmä, jolla radioaaltoalueen mittauksilla voidaan välillisesti havaita typpimonoksidin lisääntymistä 65-90 kilometrin korkeuksilla. Näin voitiin täydentää noin 50 kilometrin korkeudelle yltäviä typen oksidien satelliittihavaintoja. Näitä radioaaltomittauksia käyttäen selvitettiin vuoden 2004 keväänä pohjoisen napa-alueen stratosfäärissä satelliittimittauksilla havaittujen ennätyksellisten typenoksidi määrien alkuperäksi mesosfäärin yläpuolinen ilmakehän alue, eli termosfäärin alaosa, jossa merkittävä typen oksidien lähde ovat revontuliakin aikaansaavat varatut hiukkaset.

Väitöstyön tulokset osoittavat kuinka suuri merkitys ilmakehän ulkopuolelta tulevalla hiukkaspakotteella on ilmakehän kemiallisen tasapainon kannalta, erityisesti stratosfäärin otsonitasapainon kannalta merkittäville typen oksideille.

Julkaisijayksikkö
Kaukokartoitusyksikkö

Luokitus (UDK)
551.501, 551.590.2

Asiasanat
stratosfääri, mesosfääri, typen oksidit, otsoni, energettiset hiukkaset, hiukkassade, auringon purkaukset

ISSN ja avainnimike
0781-6117 Finnish Meteorological Institute Contributions

ISBN
978-951-697-627-6 (nid.), 978-952-10-4181-5 (PDF)

Kieli
Englanti

Myynti
Ilmatieteen laitos / Kirjasto
PL 503, 00101 Helsinki

Sivumäärä
100
Lisatietoja

Hinta

PREFACE

Several peoples contribution has been vital to this thesis work, I wish to mention a few of them.

I express my gratitude to Prof. Hannu Koskinen from Helsinki University for the inspiring tuition I experienced in space physics classes over the years, and for being the first person to suggest a research topic related to both space and atmospheric physics, which I have now fund very much my own. Conducting this work would not have been possible without continuous support from FMI in various forms: I started my Ph. D. work in the former Geophysical Research unit lead by Prof. Tuija Pulkkinen, and later continued in the then new Earth Observation unit under the leadership of Prof. Jarkko Koskinen. Over the years I have attained tremendous respect towards both of you. You have provided me with good working conditions, encouraged me in many ways, but have also been indispensable in helping me to find my place in the scientific community. I sincerely thank you for that. I am very grateful for Prof. Manuel López-Puertas from the Instituto de Astrofisica de Andalucia and Dr. Esa Turunen from the Sodankylä Geophysical Observatory for the careful examination of this thesis.

Many thanks belong my thesis adviser Prof. Erkki Kyrölä. During the course of this work, the best thing I have received from you has been the confidence and trust that I am capable of making the right decisions and that I am doing the right thing.

I wish to thank my co-authors, unofficial advisers, dear colleagues and friends Dr. Mark Clilverd and Dr. Craig Rodger from the British Antarctic Survey and the University of Otago. Your enthusiasm and wide interest in science greatly inspire me to maintain and expand mine, not to mention the excellent company you two make. It is a tremendous pleasure to work with persons who think much the same way as I do – most of the time anyway. Furthermore, I especially thank Craig for helping me to carry out my lifelong dream to visit New Zealand and Mark for introducing me to Cambridge, now one of my favourite places in the world (with and without the occasional snow), and to BAS, while in the mean time exposing me to cricket. I want to thank the whole Clilverd family for hosting me during my visits to BAS and for sharing your experiences while I was planing my first NZ visit.

During my visit to the Laboratory for Space and Atmospheric Physics at University of Colorado in 2005 is was fortunate to become acquainted with Prof. Cora E. Randall. I warmly thank you for hosting me during my visit, and for all the interest you have expressed towards my work.

Dr. Minna Palmroth and Maria Genzer, my friends and co-conspirators since the good old days at GEO, I hope you know what your friendship means to me, the words are not enough to express. I'm also indebted to Minna for helping me to find answers

to a bunch of (sometimes odd) questions concerning space physics and also for encouraging me further in my studies. The topic of this work is very interdisciplinary, as anything to do with the Sun-Earth connection always is. I have been supported both from above: the space, magnetosphere, and ionosphere, and below from the stratosphere. I particularly wanted to mention Minna, as well as Dr. Petri Toivanen, who have helped me on various issues I have had concerning the above, and Leif Backman and Laura Thölix, who have helped me with the below. I thank Dr. Johanna Tamminen and Dr. Viktoria Sofieva for many discussion concerning the use of GOMOS data and Dr. Pekka Verronen for first introducing me to the wonderful world of SPEs. In the various computer problems I have faced I have received help from many people. Most of the time the help has been near and for that I thank Seppo Hassinen. I am equally grateful for all my old friends and colleagues now at AVA and the new ones I have found at KAU for the non-work related activities. I also thank the Finnish CHAMOS group for all the fun gatherings, visits to Tähtelä, and countless excellent research plans over the recent years.

This work was fundamentally made possible by the funding received from the Academy of Finland though the *Middle Atmosphere Interactions with the Sun and Troposphere* project. Most of my visits to other institutes as well as to conferences have been enabled by the generous support I have received from the Vilho, Yrjö and Kalle Väisälä foundation/Finnish Academy of Science and Letters, the Jenny and Antti Wihuri foundation as well as the British Antarctic Survey, the Center for Space Physics/Boston University, the Sodankylä Geophysical Observatory/Oulu University and the University of Otago. I thank Tiina Tamminen and Kirsi Virolainen for patiently helping me with the more or less complicated Travel-reports.

Finally, I wish to thank my family: my parents Marja and Eero and my younger sister Anniina for continuous encouragement as well as endurance and consolation when needed. Anniina, an enormous thank you for all the craziness you have flooded my life with over the years and the shared interest in A, B, green wing and my cd collection, not to mention you ability to come up with a diversion when one is needed! In the end, my most sincere thanks belong to my late grandmother Aino Seppälä. At her time she was a strong believer in education of young women and an embodiment of female intelligence, and she always encouraged me on my path to higher education. I wish she could see me now.

Helsinki, September 2007
Annika Seppälä

CONTENTS

LIST OF ORIGINAL PUBLICATIONS

I Seppälä, Annika, Pekka T. Verronen, Erkki Kyrölä, Seppo Hassinen, Leif Backman, Alain Hauchecorne, Jean Loup Bertaux, and Didier Fussen: Solar Proton Events of October-November 2003: Ozone depletion in the Northern hemisphere polar winter as seen by GOMOS/Envisat. *Geophysical Research Letters*, 31, L19107, doi: 10.1029/2004GL021042, 2004.

II Seppälä, Annika, Pekka T. Verronen, Viktoria F. Sofieva, Johanna Tamminen, Erkki Kyrölä, Craig J. Rodger, and Mark A. Clilverd: Destruction of the Tertiary Ozone Maximum During a Solar Proton Event. *Geophysical Research Letters*, 33, L07804, doi: 10.1029/2005GL025571, 2006.

III Clilverd, Mark A., Annika Seppälä, Craig J. Rodger, Pekka T. Verronen, and Neil R. Thomson: Ionospheric evidence of thermosphere-to-stratosphere descent of polar NO_x. *Geophysical Research Letters*, 33, L19811, doi: 10.1029/2006GL026727, 2006.

IV Clilverd, Mark A., Annika Seppälä, Craig J. Rodger, Neil R. Thomson, Janos Lichtenberger, and Peter Steinbach: Temporal variability of the descent of high-altitude NO_x inferred from ionospheric data. Accepted for publication in *Journal of Geophysical Research*, doi: 10.1029/2006JA012085, 2007.

V Seppälä, Annika, Pekka T. Verronen, Mark A. Clilverd, Cora E. Randall, Johanna Tamminen, Viktoria Sofieva, Leif Backman, and Erkki Kyrölä: Arctic and Antarctic polar winter NO_x and energetic particle precipitation in 2002–2006. *Geophysical Research Letters*, 34, L12810, doi: 10.1029/2007GL029733, 2007.

In PUBL. I, PUBL. II, and PUBL. V A. Seppälä was responsible for the initial idea, the data selection and analysis, model calculations (PUBL. II) and interpretation of the results, as well as writing of the manuscripts. In PUBL. III and PUBL. IV A. Seppälä made the model calculations and selected and analysed the GOMOS data (PUBL. IV), was involved in the interpretation of the results and contributed to the writing of the manuscripts.

1 INTRODUCTION

After the British Antarctic Survey scientists discovered the ozone hole over Antarctica in 1985 [*Farman et al.*, 1985] the study of the variations in ozone content, and the different sources affecting the ozone loss, became a major concern. Ozone loss caused by Solar Proton Events was initially observed by means of rocket measurements in 1969 [*Weeks et al.*, 1972]. A few years later the relation between Solar Proton Events and atmospheric production of ozone destroying nitric oxide, NO, was identified [*Crutzen et al.*, 1975; *Heath et al.*, 1977]. Around the same time the first satellite observations of nitric oxide were made over polar regions [*Rusch and Barth*, 1975]. Over the years several studies of Solar Proton Event effects on the atmosphere have been published: The earlier work of *Crutzen and Solomon* [1980], *McPeters et al.* [1981], and *Solomon et al.* [1983] has been followed by several studies by *Jackman et al.* [*Jackman and McPeters*, 1985; *Jackman and Meade*, 1988; *Jackman et al.*, 1990; *Jackman et al.*, 1993; *Jackman et al.*, 1995, 2000], *McPeters et al.* [*McPeters and Jackman*, 1985; *McPeters*, 1986], and others [*Reid et al.*, 1991; *Callis et al.*, 1998].

Following the Solar Proton Events of October–November 2003 the severe impact that particle forcing could have on the atmosphere became of a wider interest to atmospheric scientists. Much of this was because these were the first large Solar Proton Events that occurred in the present satellite-era. For the first time continuous atmospheric observations of the particle forcing effect were available also from the nightside of the atmosphere. The Solar Proton Events which took place only a few years before, in July 2000, had not attained such a high visibility [*Jackman et al.*, 2001]. With the launch of the European Space Agency's environmental satellite Envisat in 2002, continuous observations of the polar atmospheres were at hand at the time of the 2003 events. The October–November 2003 Solar Proton Events have already led to a number of publications including PUBL. I, *von Clarmann et al.* [2005]; *Degenstein et al.* [2005]; *Jackman et al.* [2005]; *Lopéz-Puertas et al.* [2005a,b]; *Orsolini et al.* [2005]; *Randall et al.* [2005]; *Rohen et al.* [2005]; *Semeniuk et al.* [2005]; *Verronen et al.* [2005] and *Clilverd et al.* [2006b].

In the past years the scientific community has truly awoken to the importance of all different sources contributing to the ozone balance in the atmosphere and the global climate [see e.g. *Konopka et al.*, 2007]. One of these sources is the odd nitrogen produced by precipitation of energetic particles. The odd nitrogen, or NO_x, is produced at high altitudes by solar storms or by the same mechanisms that produce the beautiful high latitude aurora, and may in the course of time be transported to the stratosphere, with the aid of dynamics. In the stratosphere the odd nitrogen is able to affect the ozone balance through chemistry [*Crutzen*, 1970], a discovery which in part led to Crutzen's Nobel prize in Chemistry in 1995. The ozone changes can further lead to changes in temperature and ultimately in atmospheric dynamics. These in turn are highly important to the global climate.

As a sign of the increased understanding of the impact that high energy particle precipitation has on the composition, dynamics and chemistry of the middle atmosphere, the altitude region covering the stratosphere, mesosphere and lower thermosphere, the following *Key Scientific Questions* were, among others, posed in a Summary Report of the NASA Workshop on Sun Climate Connections held at the University of Arizona in March, 2000 [*Sprigg*, 2000]:

> *For altitudes from 35 to 120 km, what is the observed character of the odd nitrogen within and near the polar night, due to EEP (Energetic Electron Precipitation), due to auroral effects, and due to solar protons and electrons during SPEs (Solar Proton Events)?*
>
> *What is the observed flux of odd nitrogen into the stratosphere from the mesosphere during the course of a solar cycle and what is its primary source?*
>
> *Can ozone changes due to EEP, SPEs, and auroral effects alter stratospheric temperature, winds, and the phase and amplitude of the long planetary waves? In the stratosphere? In the troposphere?*
>
> *What is the importance of EEP, SPEs, and auroral effects in influencing decadal and shorter term variations of the Earth's climate? How does this variation compare with effects due to solar UV flux changes and with the effects of anthropogenic forcing?*

In order to answer these important questions, global, and especially polar, observations of ozone and odd nitrogen (NO and $\mathrm{NO_2}$ in particular) in the stratosphere–mesosphere–lower thermosphere region are needed. Since the key interests are the sources and the influence of the produced odd nitrogen, maintained in the atmosphere in the darkness of the polar night, measurement techniques capable of measuring the atmospheric composition without any sunlight present are needed. The need to see into the polar night promotes the use of stellar occultation technique, previously not been extensively used in satellite observations, over the widely used solar occultation and limb scattering techniques. In order to study the possible effects on climate, the observations must extend over long periods of time, long meaning several years, even decades. This would be required also in the case of resolving the odd nitrogen production throughout the solar cycle.

In this work several of the questions raised by the NASA workshop have been addressed. The main emphasis is the effect of Solar Proton Events, as well as energetic particle precipitation in general, on odd nitrogen in the middle atmosphere. This has mainly been done with the aid of observations performed by the GOMOS instrument originally proposed by Finland, France and Belgium, on board the European Space Agency's Envisat satellite launched in 2002. The full name of the instrument, which was first proposed to the European Space Agency in 1988, is Global Ozone Monitoring

by Occultation of Stars. Among other species, GOMOS measures O_3 and NO_2 in the stratosphere and mesosphere with global coverage.

This work is composed of five original publications listed on page 8. The results of these publications are summarised on page 44. The chemistry related to the ozone balance of the middle atmosphere and to this work is presented in Chapter 2. Chapter 2 also includes a general description of the dynamics and vertical and horizontal transport in the polar atmosphere, most relevant regarding the results presented later. In Chapter 3 two measurement techniques are introduced: that of the GOMOS instrument and the subionospheric Very Low Frequency (VLF) radio wave propagation. These are then utilised in the observation of energetic particle induced effects on the atmospheric composition which are presented in Chapter 4. The sources of the precipitating energetic particles and the coupling mechanism of the particles with the atmosphere are also discussed. Summary of the results as well as concluding remarks and discussion on some future prospects are given in Chapter 5.

2 CHEMISTRY AND DYNAMICS

This chapter presents the chemistry related to the ozone balance in the upper-stratosphere and mesosphere. After the introduction of pure oxygen chemistry, the role of odd nitrogen and odd hydrogen in the ozone balance are discussed. Other gases relevant to the general ozone balance in the stratosphere [see $e.g.$ *Brasseur and Solomon*, 2005], such as chlorine and bromine species, which are not known to be significantly perturbed by energetic particle precipitation, are not considered here in detail. Extensive reviews on atmospheric chemistry are provided in, *e.g.*, *Seinfeld and Pandis* [1998], *Finlayson-Pitts and Pitts* [1999], and *Brasseur and Solomon* [2005].

As the distribution of minor constituents in the middle atmosphere (from about 20 km to about 100 km) is affected by both chemical and dynamical processes, a general description of the dynamics and transport processes in the polar atmosphere, to which this work emphasises on, are given in section 2.2.

2.1 OZONE AND RELATED CHEMISTRY IN THE MIDDLE ATMOSPHERE

In the middle atmosphere chemistry related to ozone is frequently regarded through the odd oxygen family, denoted O_x. This family consists of the oxygen ground state $\mathrm{O}(^3\mathrm{P})$, the first exited state $\mathrm{O}(^1\mathrm{D})$, and O_3, the ozone molecule,

$$\mathrm{O}_x = \mathrm{O}(^3\mathrm{P}) + \mathrm{O}(^1\mathrm{D}) + \mathrm{O}_3.$$

Figure 2.1 presents the main reactions within the odd oxygen family. The main reactions producing atomic oxygen are UV photodissociation of O_2

$$\mathrm{O}_2 \xrightarrow{\mathrm{h}\nu} 2\mathrm{O}, \tag{2.1}$$

and photodissociation of O_3

$$\mathrm{O}_3 \xrightarrow{\mathrm{h}\nu} \mathrm{O}_2 + \mathrm{O}, \tag{2.2}$$

producing either the ground state $\mathrm{O}(^3\mathrm{P})$ ($\geq$ 320 nm) or the first excited states, *e.g.* $\mathrm{O}(^1\mathrm{D})$ ($\leq$ 320 nm) of O, depending on the photon wavelength. Ozone is formed solely in the reaction

$$\mathrm{O} + \mathrm{O}_2 \xrightarrow{\mathrm{M}} \mathrm{O}_3. \tag{2.3}$$

O_x loss mechanisms include

$$\mathrm{O} + \mathrm{O} \xrightarrow{\mathrm{M}} \mathrm{O}_2 \tag{2.4}$$

and

$$\mathrm{O} + \mathrm{O}_3 \xrightarrow{\mathrm{M}} 2\mathrm{O}_2 \tag{2.5}$$

The three body reactions 2.4 and 2.5 require the presence of either N_2 or O_2 molecules (M) to take place and are thus pressure dependent. With the decreasing pressure in

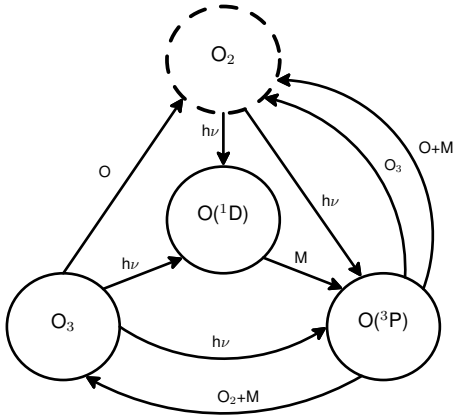

FIGURE 2.1. Main chemical reactions of the O_x-compounds (Based on Fig. 5.1 of *Shimazaki* [1984]). The dashed circle represents O_x source molecule. Note that photodissociation of O_3 also produces O_2 (2.2).

the upper mesosphere and lower thermosphere these reactions become slow, resulting in larger abundance and longer lifetime of O at high altitudes compared with lower altitudes. During nighttime there is no production of O (2.1, 2.2), but atomic oxygen is converted to O_3 by the fast reaction (2.3). This results in higher abundance of O_3 during nighttime in the mesosphere and lower thermosphere, whereas in the stratosphere the diurnal variation of O_3 is negligible due to the short chemical lifetime of atomic oxygen.

2.1.1 NO_x chemistry

The NO_x gases N, NO, and NO_2 are formed primarily in the stratosphere through the the reaction $N_2O + O(^1D) \rightarrow 2NO$, and in the thermosphere through both photodissociation and photoionisation of N_2. Precipitating charged particles produce NO_x through ionisation or dissociative ionisation of N_2 and O_2 molecules, which results in the formation of N_2^+, O_2^+, N^+, O^+, and NO^+. The reactions of these ions lead to formation of both the excited nitrogen atoms $N(^2D)$ and the ground state of nitrogen $N(^4S)$ [*Rusch et al.*, 1981; *Solomon et al.*, 1982]:

$$N_2^+ + O \rightarrow NO^+ + N \tag{2.6}$$

$$N_2^+ + e^- \rightarrow N + N \tag{2.7}$$

$$O^+ + N_2 \rightarrow NO^+ + N \tag{2.8}$$

$$N^+ + O_2 \rightarrow O^+ + NO \rightarrow NO^+ + O \rightarrow O_2^+ + N \tag{2.9}$$

$$NO^+ + e^- \rightarrow N + O. \tag{2.10}$$

Almost all of the excited nitrogen $N(^2D)$ further reacts with O_2 to form NO in the reaction

$$N + O_2 \rightarrow NO + O, \tag{2.11}$$

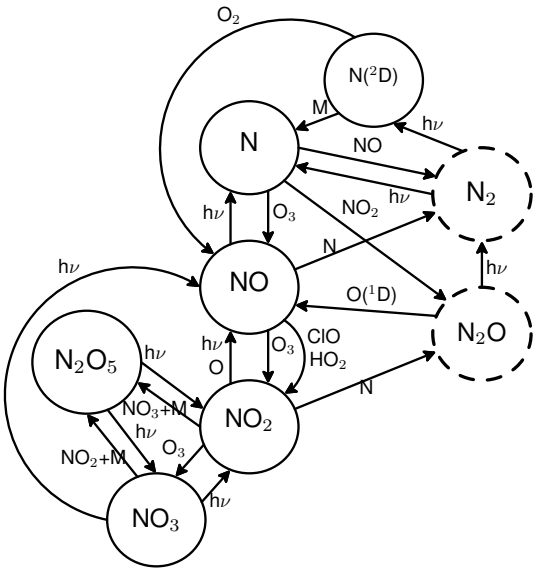

FIGURE 2.2. Main chemical reactions of the NO_x-compounds (Based on Fig. 5.4 of *Shimazaki* [1984]). The dashed circles represent NO_x source molecules.

providing a significant pathway to NO production. The produced NO is converted into NO_2 in various reactions (mainly in reaction 2.16) [see *e.g. Brasseur and Solomon*, 2005, pp. 336-341], but the formed NO_2 is quickly converted back to NO either in reaction with O

$$\mathrm{NO}_2 + \mathrm{O} \rightarrow \mathrm{NO} + \mathrm{O}_2, \tag{2.12}$$

or by photolysis

$$\mathrm{NO}_2 \xrightarrow{\mathrm{h}\nu} \mathrm{NO} + \mathrm{O}(^3\mathrm{P}). \tag{2.13}$$

During nighttime, when little O is available, and the above reactions are ineffective, all NO is rapidly converted to NO_2 after sunset.

In the upper stratosphere and above, the loss of NO is mainly through photodissociation

$$\mathrm{NO} \xrightarrow{\mathrm{h}\nu} \mathrm{N}(^4\mathrm{S}) + \mathrm{O}, \tag{2.14}$$

at wavelengths shorter than 191 nm, followed by

$$\mathrm{N}(^4\mathrm{S}) + \mathrm{NO} \rightarrow \mathrm{N}_2 + \mathrm{O}, \tag{2.15}$$

known as the cannibalistic loss, where two NO molecules are lost per absorbed photon. Some of the main reactions within the NO_x family are presented in Figure 2.2.

The nitrogen compounds are an important factor in catalytic ozone loss in the stratosphere. NO_x cycles which lead to ozone destruction but leave the NO_x compounds intact are:

$$\mathrm{NO} + \mathrm{O_3} \rightarrow \mathrm{NO_2} + \mathrm{O_2} \tag{2.16}$$
$$\mathrm{NO_2} + \mathrm{O} \rightarrow \mathrm{NO} + \mathrm{O_2} \tag{2.17}$$
$$\text{Net: } \mathrm{O} + \mathrm{O_3} \rightarrow 2\mathrm{O_2}$$

$$\mathrm{NO} + \mathrm{O_3} \rightarrow \mathrm{NO_2} + \mathrm{O_2} \tag{*2.16}$$
$$\mathrm{NO_2} + \mathrm{O_3} \rightarrow \mathrm{NO_3} + \mathrm{O_2} \tag{2.18}$$
$$\mathrm{NO_3} \xrightarrow{\mathrm{h}\nu} \mathrm{NO} + \mathrm{O_2} \tag{2.19}$$
$$\text{Net: } 2\mathrm{O_3} \rightarrow 3\mathrm{O_2}$$

and

$$\mathrm{NO} + \mathrm{O_3} \rightarrow \mathrm{NO_2} + \mathrm{O_2} \tag{*2.16}$$
$$\mathrm{NO_2} + \mathrm{O_3} \rightarrow \mathrm{NO_3} + \mathrm{O_2} \tag{*2.18}$$
$$\mathrm{NO_2} + \mathrm{NO_3} \xrightarrow{\mathrm{M}} \mathrm{N_2O_5} \tag{2.20}$$
$$\mathrm{N_2O_5} \xrightarrow{\mathrm{h}\nu} \mathrm{NO_3} + \mathrm{NO_2} \tag{2.21}$$
$$\mathrm{NO_3} \xrightarrow{\mathrm{h}\nu} \mathrm{NO} + \mathrm{O_2} \tag{*2.19}$$
$$\text{Net: } 2\mathrm{O_3} \rightarrow 3\mathrm{O_2}$$

In the absence of energetic particle precipitation, photoionisation of NO by the solar Lyman-α radiation at 121.6 nm provides the main source of electrons in the mesosphere and lower thermosphere. This also leads to the formation of the ionospheric D layer located between about 50 and 100 km. The solar Lyman-α radiation scattered from the hydrogen geocorona is also an important source of ionisation in the nighttime D region. Because of the direct connection between the amount of NO and the electron density, measurement techniques, such as radio waves, utilising the D-layer electrons may be used to indirectly observe changes in the NO density in the D layer (see section 3.2).

Polar night NO_x

As was noted earlier, in the middle atmosphere below about 70 km NO is rapidly converted to $\mathrm{NO_2}$ after sunset. Above about 70 km altitude, however, the photochemical lifetime of $\mathrm{NO_2}$ is only of the order of seconds in both day and night conditions (reactions 2.16, 2.12, 2.13, and 2.18) [*Shimazaki*, 1984]. Thus NO_x (or the more extensive odd nitrogen family NO_y (N + NO + $\mathrm{NO_2}$ + $\mathrm{NO_3}$ + $2\mathrm{N_2O_5}$ + $\mathrm{HNO_3}$ + $\mathrm{HO_2NO_2}$ + $\mathrm{ClONO_2}$ + $\mathrm{BrONO_2}$)), is mainly in the form of (N + NO) in the mesosphere and above [*Brasseur and Solomon*, 2005, pp. 328].

2.1.2 *HO_x chemistry*

The hydrogen radicals, H, OH, and HO_2, denoted as HO_x, are highly reactive gases and important to the odd oxygen balance particularly in the mesosphere. The main source of HO_x in the mesosphere and above is the (UV) photolysis of water vapour. In the stratosphere and lower mesosphere HO_x is formed in the reaction of water vapour with the $O(^1D)$ atom. HO_x is also produced through precipitation of energetic particles: The initial production of ion pairs is followed by formation and reactions of water cluster ions which result in the production of HO_x. The complex ion chemistry involved in this process is discussed *e.g.* by *Solomon et al.* [1981] and is briefly presented below.

The produced O_2^+ ions react to form $O_2^+ \cdot H_2O$ ions through

$$O_2^+ + O_2 \xrightarrow{M} O_4^+ \tag{2.22}$$
$$O_4^+ + H_2O \rightarrow O_2^+ \cdot H_2O + O_2. \tag{2.23}$$

The formed hydrate ions then further react in one of the following cycles to produce HO_x:

$$O_2^+ \cdot H_2O + H_2O \rightarrow H_3O^+ \cdot OH + O_2 \tag{2.24}$$
$$H_3O^+ \cdot OH + e^- \rightarrow H + OH + H_2O \tag{2.25}$$
$$\text{Net: } H_2O \rightarrow H + OH,$$

or

$$O_2^+ \cdot H_2O + H_2O \rightarrow H_3O^+ \cdot OH + O_2 \tag{2.26}$$
$$H_3O^+ \cdot OH + H_2O \rightarrow H_3O^+ \cdot H_2O + OH \tag{2.27}$$
$$H_3O^+ \cdot H_2O + nH_2O \rightarrow H_3O^+(H_2O)_{n+1} \tag{2.28}$$
$$H_3O^+(H_2O)_{n+1} + e^- \rightarrow H + (n+2)H_2O \tag{2.29}$$
$$\text{Net: } H_2O \rightarrow H + OH,$$

or

$$O_2^+ \cdot H_2O + H_2O \rightarrow H^+ \cdot H_2O + OH + O_2 \tag{2.30}$$
$$H^+ \cdot H_2O + nH_2O \rightarrow H_3O^+(H_2O)_n \tag{2.31}$$
$$H_3O^+(H_2O)_n + e^- \rightarrow H + (n+1)H_2O \tag{2.32}$$
$$\text{Net: } H_2O \rightarrow H + OH.$$

The HO_x radicals are very reactive and thus have a very short chemical lifetime in the atmosphere; below 80 km the lifetime of the HO_x family is of the order of minutes to hours. As a result, the HO_x distribution is independent of transport processes. Above 80 km the chemical lifetime of HO_x increases but because of the low abundance of water vapour the concentration of HO_x at these altitudes is also small.

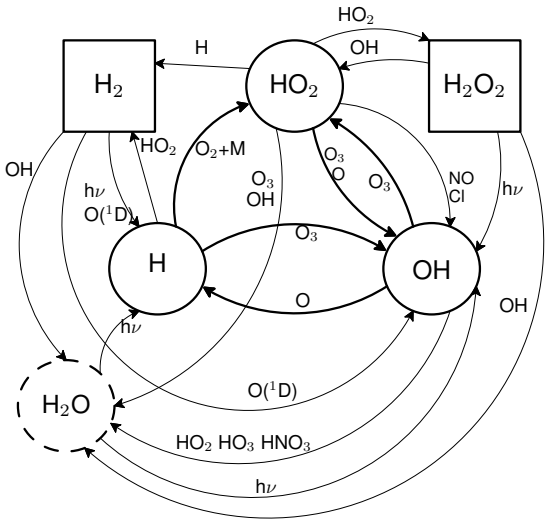

FIGURE 2.3. Main chemical reactions of the HO_x-compounds (Based on Fig. 5.3 of *Shimazaki* [1984]). The dashed circles represent HO_x source molecules and the boxes HO_x reservoirs.

The catalytic HO_x cycles affect the ozone balance mainly in the upper stratosphere and above because they include reactions with atomic oxygen. Some of the reactions within the HO_x family are shown in Figure 2.3. The most important catalytic cycles destroying odd oxygen are:

$$\mathrm{H} + \mathrm{O}_2 \xrightarrow{\mathrm{M}} \mathrm{HO}_2 \tag{2.33}$$
$$\mathrm{HO}_2 + \mathrm{O} \rightarrow \mathrm{OH} + \mathrm{O}_2 \tag{2.34}$$
$$\mathrm{OH} + \mathrm{O} \rightarrow \mathrm{H} + \mathrm{O}_2 \tag{2.35}$$
$$\text{Net: } 2\mathrm{O} \rightarrow \mathrm{O}_2,$$

and

$$\mathrm{H} + \mathrm{O}_3 \rightarrow \mathrm{OH} + \mathrm{O}_2 \tag{2.36}$$
$$\mathrm{OH} + \mathrm{O} \rightarrow \mathrm{H} + \mathrm{O}_2 \tag{*2.35}$$
$$\text{Net: } \mathrm{O} + \mathrm{O}_3 \rightarrow 2\mathrm{O}_2$$

These rapid reaction cycles participate in ozone loss above 40 km.

Other HO_x reaction cycles effecting O_x in the middle and upper stratosphere and mesosphere are:

$$\mathrm{OH} + \mathrm{O}_3 \rightarrow \mathrm{HO}_2 + \mathrm{O}_2 \tag{2.37}$$
$$\mathrm{HO}_2 + \mathrm{O} \rightarrow \mathrm{OH} + \mathrm{O}_2 \tag{*2.34}$$
$$\text{Net: } \mathrm{O} + \mathrm{O}_3 \rightarrow 2\mathrm{O}_2,$$

and

$$\mathrm{OH + O \rightarrow H + O_2} \quad \text{(*2.35)}$$
$$\mathrm{H + O_2 \xrightarrow{M} HO_2} \quad \text{(*2.33)}$$
$$\mathrm{HO_2 + O_3 \rightarrow OH + 2O_2} \quad \text{(2.38)}$$
$$\text{Net: } \mathrm{O + O_3 \rightarrow 2O_2}$$

2.1.3 Halogen chemistry

Reactions with halogen compounds, chlorine, fluorine, bromine, and iodine, are important to stratospheric ozone balance in general. The source of halogens is the release of halocarbons from the surface from where they are transported through the troposphere to the stratosphere, where they break up and release the halogens. The released Cl, F, and Br rapidly react with ozone to form ClO, FO and BrO. The ClO_x (Cl + ClO) and BrO_x (Br + BrO) compounds destroy O_x in catalytic reaction cycles like those of the NO_x and HO_x species:

$$\mathrm{X + O_3 \rightarrow XO + O_2} \quad \text{(2.39)}$$
$$\mathrm{XO + O \rightarrow X + O_2} \quad \text{(2.40)}$$
$$\text{Net: } \mathrm{O + O_3 \rightarrow 2O_2}$$

and

$$\mathrm{X + O_3 \rightarrow XO + O_2} \quad \text{(*2.39)}$$
$$\mathrm{XO + HO_2 \rightarrow HOX + O_2} \quad \text{(2.41)}$$
$$\mathrm{HOX \xrightarrow{h\nu} X + OH} \quad \text{(2.42)}$$
$$\mathrm{OH + O_3 \rightarrow HO_2 + O_2} \quad \text{(*2.37)}$$
$$\text{Net: } \mathrm{2O_3 \rightarrow 3O_2}$$

where X may be either Cl or Br. For chlorine ($\mathrm{X = Cl}$), the first of these cycles is important to the ozone balance of the upper stratosphere. The latter cycle is more important near 20 km altitude. Several other reaction cycles affecting ozone in the lower stratosphere, as well as chemistry related to chlorine activation in the presence of polar stratospheric clouds, are presented in $e.g.$ *Brasseur and Solomon* [2005]. Chlorine species have been found to be affected during Solar Proton Events when the amount of HO_x in the middle atmosphere has increased [*Lopéz-Puertas et al.*, 2005b; *von Clarmann et al.*, 2005]. These effects are discussed later in section 4.2.

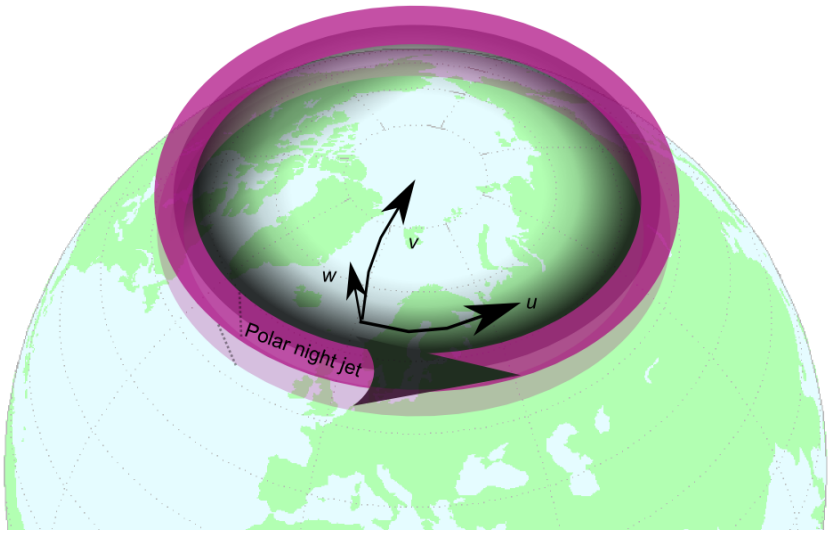

FIGURE 2.4. Approximate location of the Northern Hemisphere Polar Night Jet, inside which the polar vortex is formed, and the wind vector directions (zonal u, meridional v and vertical w).

2.2 DYNAMICS AND TRANSPORT

This section gives a general description of the dynamical and transport processes in the middle atmosphere. As this work is focused on the polar areas, more attention is paid to the processes characteristic of the polar atmosphere.

In the winter polar middle atmosphere transport is largely determined by the polar vortex. In the winter pole, near the polar night terminator, strong temperature gradients lead to formation of the Polar Night Jet. As shown in Figure 2.4, the Polar Night Jet is a strong eastward (westerly) wind in the upper stratosphere-lower mesosphere near 60°N/S latitude, formed due to the thermal wind balance [*Solomon*, 1999; *Holton*, 2004]. The winds in the Polar Night Jet, which reach their peak of about 80 m/s near 60 km altitude, act as a transport barrier between polar and mid-latitude air, blocking meridional transport and isolating the air in the polar stratosphere and thus forming the polar vortex. The edge of the vortex is usually near 60°N/S and it extends from approximately 16 km to the mesosphere. The isolation is greater, and the polar vortex more stable, in the Antarctic where there is less wave activity affecting the vortex than in the Arctic. In the Arctic, the atmospheric wave activity disturbs the vortex, leading to greater mixing and faster downward motion, compared with those in the Antarctic vortex [*Solomon*, 1999]. The approximate location of the Polar Night Jet is presented in Figure 2.4 and the approximate location of the edge of the polar vortex in Figure 2.5.

The large-scale meridional circulation in the stratosphere is determined by the Brewer-Dobson circulation. The Brewer-Dobson circulation is formed by rising motion from the troposphere to the stratosphere in the tropics, poleward transport at strato-

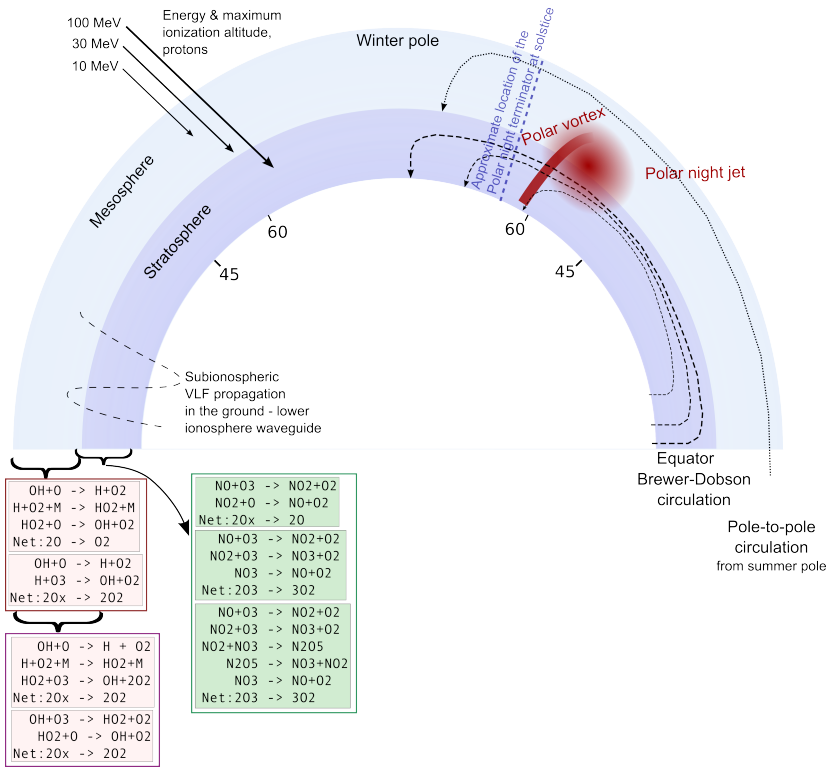

FIGURE 2.5. Different phenomena in the winter pole middle atmosphere. On the left side are presented phenomena related to ionisation by precipitating protons, subionospheric radio wave propagation and catalytic reaction cycles of the HO_x and NO_x gases. Also shown are the altitudes regions where the cycles are effective (as indicated by the curly brackets). On the right are shown phenomena related to dynamics. The approximate location of the polar night jet is presented as red circle and the darker colour indicates the area where the peak winds are observed. The red curve depicts the approximate location of the polar vortex. Location of latitudes 45° and 60° are indicated with the respective numbers.

spheric altitudes and sinking motion at mid- and high latitudes. In the mesosphere, the meridional circulation is formed by a single cell in which rising motion takes place in the summer pole starting from the stratosphere, pole-to-pole transport in mesosphere-lower-thermosphere, and downward motion in the winter pole mesosphere, down to the stratosphere.

An important factor to be taken into account in the atmospheric dynamics is the effect of waves. Atmospheric waves are also the main driver of the mean circulation [*Salby and Callaghan*, 2006]. Planetary (*i.e.* Rossby) and gravity waves affect both vertical and horizontal transport and may induce great transient deviations from observed mean values. Gravity waves, which are formed from vertical displacement of air parcels, are highly important for mesospheric dynamics but less important in the stratosphere. The waves break at mesospheric altitudes, where the wave amplitude

has grown so large that the vertical temperature perturbation results in the air parcels becoming convectively unstable *i.e.* they break. In the mesosphere gravity waves propagate mainly westward in the winter and eastward during summer. Large-scale planetary (Rossby) waves are induced by orography and land-sea distribution. These waves propagate westward (with respect to the mean flow), upwards (on westerly mean zonal wind), and equatorwards and propagate in the stratosphere mainly during wintertime [*Holton*, 2004; *Brasseur and Solomon*, 2005]. Breaking Rossby waves causes rapid irreversible mixing of the air parcels. Sudden Stratospheric Warming events, which are mainly observed in the Northern Hemisphere, arise from enhanced propagation of planetary waves from the troposphere to the stratosphere. These events are marked by the polar vortex becoming highly distorted and finally breaking down with accompanying warming of the polar stratosphere leading to formation of easterly circumpolar flow [*Holton*, 2004]. The sudden warming of the polar stratosphere arises from strong downward motion taking place in the polar region and simultaneous upward motion in the tropics. After the warming event the polar vortex is generally restored, and occasionally becomes exceptionally strong as in the Northern Hemisphere in February–March 2004 [*Manney et al.*, 2005]. Sudden Stratospheric Warmings have also been shown to be associated with mesospheric cooling events [*Siskind et al.*, 2005].

2.2.1 Horizontal transport

Horizontal transport in the stratosphere and mesosphere is determined by winds in the zonal (longitudinal, u) and meridional (latitudinal, v) directions as presented in Figure 2.4. In the polar winter stratosphere the mean zonal winds are in general directed eastwards (westerlies) along with the polar night jet. At higher altitudes the zonal winds remain westerly up to about 90 km altitude above which the wind direction is reversed [*Brasseur and Solomon*, 2005]. The mean wintertime zonal wind speeds are tens of meters per second throughout the middle atmosphere. The mean meridional circulation in the winter pole is driven by the Brewer-Dobson circulation and with wind speeds of a few m/s is slow compared to the mean zonal wind. However as the wave activity, particularly in the winter hemisphere, may influence the direction of the wind flow, winds in the meridional direction may increase substantially [*Holton*, 2004; *Brasseur and Solomon*, 2005].

2.2.2 Descent of air in the polar vortex

Inside the polar vortex the descent varies from year to year but also with respect to the distance from the vortex edge and altitude [*Manney et al.*, 1994; *Rosenfield and Schoeberl*, 2001]. The wintertime descent is known to be more rapid in the vortex core (compared to the vortex edge) at the beginning of the winter in the northern hemisphere and generally more rapid at high altitudes than at lower altitudes. *Callaghan*

and Salby [2002] have shown from model simulations that, in general, the maximum descent rates in the wintertime Northern Hemisphere middle and upper stratosphere are found near 60° latitude (2 mm/s), and not over the pole (1.8 mm/s). At lower altitudes the descent is slower, with vertical descent rates of 0.4-0.7 mm/s (1.2-1.8 km/month) in the Antarctic middle stratosphere [*Kawamoto and Shiotani*, 2000]. In the lower stratosphere mean downwelling rates are of the order of 1 mm/s but increase to several mm per second in the mesosphere [*Callaghan and Salby*, 2002]. Model simulations of *Rosenfield et al.* [1994] have shown that in both hemispheres the descent rates increase markedly with height due to increasing cooling rates. At higher altitudes there is also significant variability: In the Arctic, air parcels initialised at 50 km altitude at the beginning of November descent 27 km in less than five months (on average 6 km/month), whereas parcels initiated at the same level in January experience the same descent in under three months (on average 9 km/month). In the Antarctic air parcels initialised at 52 km in March descended 26-29 km in under eight months (on average 3.4 km/month). Those initialised in July reach the same final altitudes in only four months (on average 6.9 km/month), descending 14 km in the first month alone.

In the NH, where the polar vortex is more disturbed than in the SH, there is more year to year variation in the descent, as changes in the wave activity and frequently occurring stratospheric warmings affect the vortex conditions [*Rosenfield and Schoeberl*, 2001; *Brasseur and Solomon*, 2005]. Calculating the fraction of upper stratospheric and mesospheric air in the spring time polar vortex during polar winters of 1992–2000, *Rosenfield and Schoeberl* [2001] found that up to 90 % of stratospheric air originated from above 45 km, unless unusually late vortex formation (NH and SH) or major stratospheric warmings (NH) occurred. As a result of late vortex formation or major stratospheric warming only a small fraction (less than 10 %) of stratospheric air was found to be of high altitude origin.

2.2.3 Transport and chemical lifetimes

The photochemical lifetime (e-folding lifetime, photochemical time constant) of species X, τ_{chem}, is the time required for the concentration of X to decrease to $1/e$ of the initial concentration [*Brasseur and Solomon*, 2005]. The time constant for transport (dynamical processes) τ_{dyn} (time required for the concentration of X to decrease to $1/e$ of the initial concentration as a result of transport by winds) can be similarly derived. Table 2.1 presents approximate photochemical lifetimes of the O_x, NO_x, and HO_x families and τ_{dyn} for zonal, meridional, and vertical winds at four different altitudes. Whenever the chemical lifetime exceeds that of transport, the constituent is under dynamical control. In the opposite situation the constituent is under photochemical equilibrium. If the timescales are comparable, both processes must be considered.

Table 2.1 Photochemical lifetimes and transport timescales at middle atmospheric altitudes. Based on results presented by *Brasseur and Solomon* [2005]. When different from the photochemical time constants, the nighttime chemical time constants based on *Shimazaki* [1984] are given in brackets (NO_x family then including N_2O_5 and HNO_3).

	Component	40 km	60 km	80 km	100 km
τ_{chem}	O_x	1 day (year)	1 hour (year)	5 hours (day)	1 month (month)
	NO_x	1 month (years)	1 month (years)	1 month (years)	2 days (years)
	HO_x	minutes	1 hour	1 day	100 years
τ_{dyn}	Zonal wind	12 hours	12 hours	1 day	1 day
	Meridional wind	1 month	10 days	2 days	10 days
	Vertical wind	2 months	1 month	4 months	4 months

2.3 VERTICAL DISTRIBUTION OF OZONE

The amount of ozone at any altitude is determined by the balance between ozone production, ozone loss and transport. This can be expressed using the continuity equation

$$\frac{\partial n_i}{\partial t} + \nabla \cdot n_i \mathbf{v} = S_i \tag{2.43}$$

where n_i is the density of species i, $\mathbf{v}$ is the wind vector and S_i is the net chemical source term. The net source term may also be expressed as

$$S_i = P_i - L_i n_i, \tag{2.44}$$

where P_i is the production term and $L_i n_i$ is the loss term.

As was written in section 2.1 ozone formation in the atmosphere takes place through reaction

$$\mathrm{O} + \mathrm{O_2} \xrightarrow{\mathrm{M}} \mathrm{O_3}, \tag{*2.3}$$

while ozone loss happens through several different reactions including those within the O_x family and those initiated by the NO_x and HO_x gases as presented in section 2.1. Therefore the production term P_i is determined by the rate of the reaction 2.3 and the atomic oxygen abundance.

The examination of the vertical ozone profile in the 20 km to 100 km altitude region reveals that the ozone profile is dominated by three local ozone maxima, as shown in Figure 2.6. The first ozone maximum is observed at around 30 km and is called the primary ozone maximum. If the ozone profile is viewed in absolute densities instead of mixing ratios, the primary maximum is located at lower altitudes at around 15 to 26 km. This ozone maximum is formed in conditions where molecular oxygen is photolysed by radiation in the ultraviolet wavelength range (200 nm to 242 nm, also called the Hertzberg continuum) leading to production of atomic oxygen, which is then used in ozone formation in reaction 2.3 [*Brasseur and Solomon*, 2005].

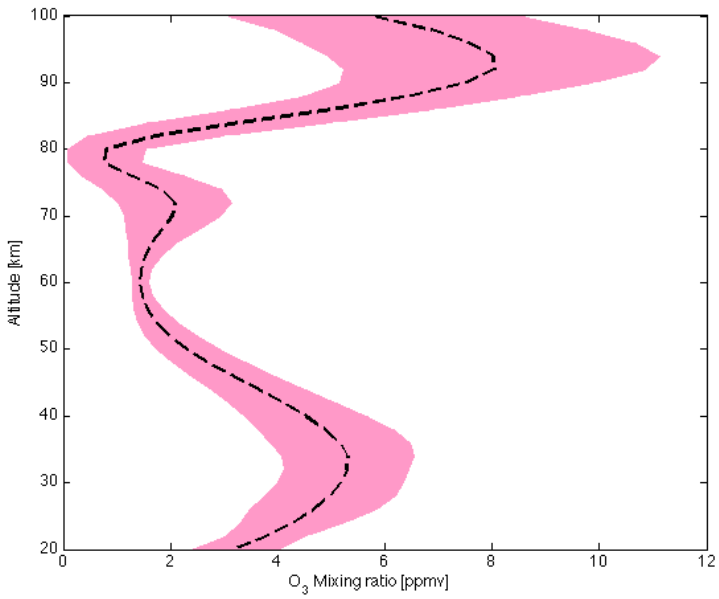

FIGURE 2.6. Sample nighttime ozone profile showing the three local ozone maxima: The primary ozone maximum around 30 km altitude, secondary maximum around 90 km and the tertiary ozone maximum around 70 km altitude. The black dashed line is the average nighttime ozone profile in the Northern Hemisphere polar area (latitudes 60°–90°) calculated from GOMOS measurements over the year 2003. The light red shaded area represents the standard deviation of the measurements. The amount of ozone is presented in volume mixing ratios (VMR). Volume mixing ratio is a dimensionless variable that presents the fraction of a given substance in the studied air volume (density of substance/total density of air). In the atmosphere, ozone mixing ratios are frequently presented in terms of parts per million volume, ppmv.

The secondary ozone maximum is observed near the mesopause at altitudes around 80 km to 90 km in absolute densities, and around 90 km altitude in volume mixing ratios (as presented in Figure 2.6). This maximum arises from atomic oxygen formation from O_2 photolysis by the far ultraviolet radiation in the Schuman Runge continuum and Schuman Runge bands at wavelengths 130–175 nm and 175–200 nm respectively [*Brasseur and Solomon*, 2005], and downward transport of atomic oxygen from the thermosphere.

The tertiary ozone maximum observed most pronouncedly in ozone mixing ratio profile around 70 km altitude does not originate from increase in the production term as the first and the second maximum. The tertiary maximum which is observed close to the polar night terminator, is rather due to combination of decrease in atomic oxygen loss [*Marsh et al.*, 2001] and atmospheric dynamics [*Hartogh et al.*, 2004]. *Marsh et al.* [2001] proposed that the ozone maxima occurs near the polar night terminator

around 72 km altitude as a result of less HO_x production from reduced water vapour photolysis, which decreases with increasing solar zenith angles in the polar night terminator area. In the conditions when the tertiary ozone maximum occurs, water vapour photolysis has significantly decreased but shorter wavelength radiation is still able to produce atomic oxygen thus providing ozone production source. Using a three dimensional model of the middle atmosphere *Hartogh et al.* [2004] found that, although the two phenomena are chemically separate, the tertiary maximum is connected by dynamics to the ozone minimum observed around 80 km altitude. They also found that, as meridional wind transports the air from the polar night terminator area to the polar night domain, the efficiency of chemical reactions is changed due to the odd oxygen distribution of the tertiary ozone maximum and the ozone minimum.

2.4 VERTICAL DISTRIBUTION OF NO_x

Figure 2.7 shows the vertical distribution of several NO_x family species calculated by ion and neutral chemistry model. The profiles are shown for both noon and midnight. The upper figure represents situation when no additional ionisation source is present, the lower figure the situation during a moderate Solar Proton Event, with ionisation from proton precipitation. The figure shows the strong diurnal variation of the individual NO_x gases while the total NO_x has only small diurnal variation. During daytime, above about 50 km the main NO_x component is NO while during nighttime the amount of NO decreases below about 70 km and NO_2 becomes a significant NO_x component.

In the lower thermosphere, where a NO_x maximum is observed, NO_x is formed through dissociation and ionisation of N_2, either by solar radiation or by energetic particles, which are an important source of NO_x in the lower thermosphere. From the lower thermosphere the produced NO_x is transported downwards to the mesosphere. Another NO_x maximum is located in the stratosphere. There the main source of NO_x is the oxidation of N_2O. Between the two maximums a local minimum is located at around altitude 80 km. This minimum is a result of photolysis of NO (2.14) at wavelengths $<$191 nm, and the following recombination of the produced nitrogen atom with NO (2.15) [*Siskind*, 2000].

The strong diurnal variation of NO and NO_2 seen in Figure 2.7 is mainly due to the rapid conversion of NO to NO_2 after sunset as discussed in section 2.1.1. During nighttime NO_2 also reacts with atomic oxygen produce NO_3, which is photolysed back to NO_2 during day by radiation at wavelengths $<$620 nm. During daytime NO_2 is photolysed to NO ($<$405 nm) or reacts with O to form NO.

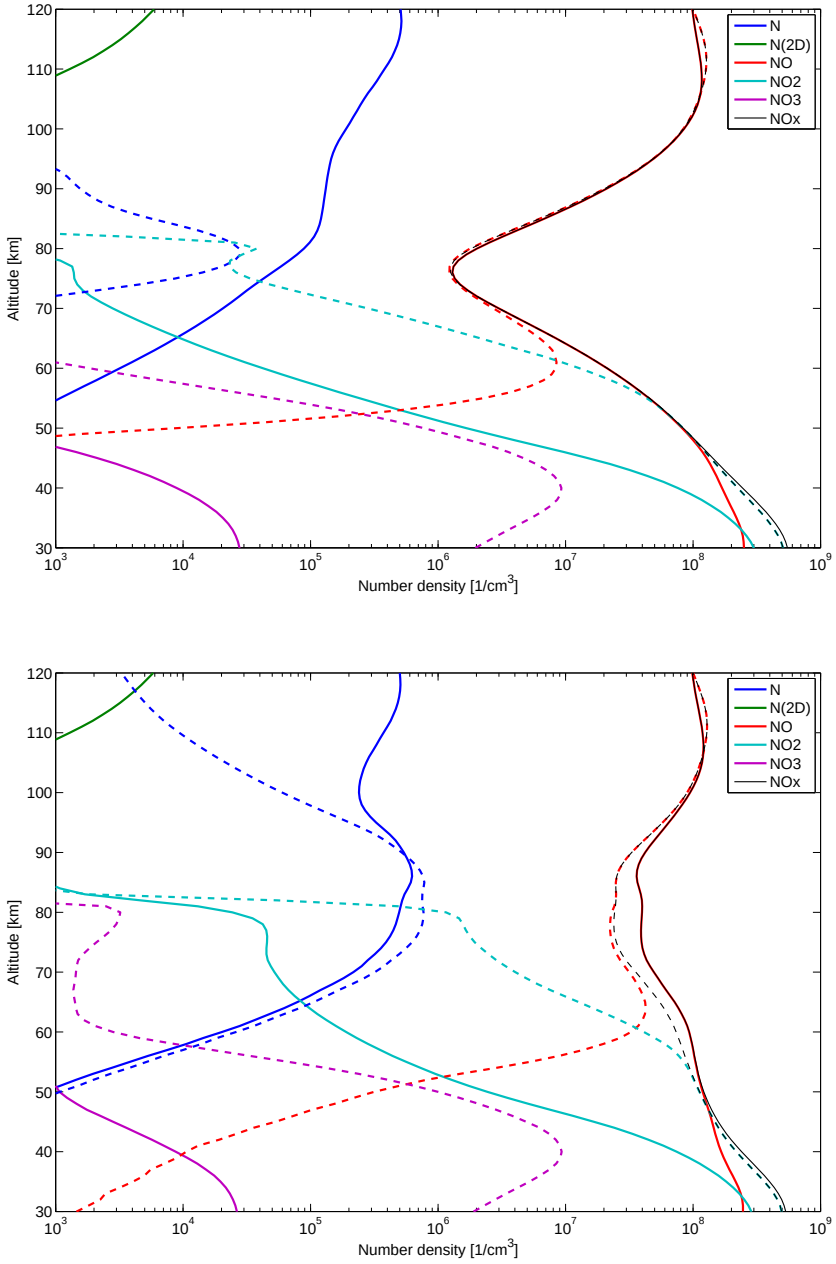

FIGURE 2.7. Sample odd nitrogen (N, $N(^2D)$, NO, NO_2, NO_3, and NO_x ($NO+NO_2$)) profiles from the Sodankylä Ion Chemistry model. The profiles have been calculated for latitude 70°N and for September. The solid lines correspond to noon conditions and the dashed lines to midnight. The upper figure represents conditions with no additional ionisation source from energetic particle precipitation. The lower figure shows how the NO_x profiles were affected by a moderate Solar Proton Event in September 11th, 2005.

3 MEASUREMENTS

This Chapter presents the two measurement techniques used later in the observation of energetic particle precipitation effects on the middle atmosphere. First, in section 3.1, is presented the GOMOS instrument that observes chemical composition of the middle atmosphere. In section 3.2 is presented the subionospheric radio wave propagation technique, used for monitoring changes in the ionisation of mesosphere-lower thermosphere region.

3.1 THE GOMOS INSTRUMENT

Global Ozone Monitoring by Occultation of Stars (GOMOS) is a stellar occultation instrument on board the European Space Agency's Envisat satellite, shown in Figure 3.1 [*Bertaux et al.*, 1991, 2004; *Kyrölä et al.*, 2004]. The Envisat satellite was launched on March 2002 with the main objective to provide information for studying and monitoring the Earth and its environment. The satellite carries a total of ten instruments, three (GOMOS, MIPAS, and SCIAMACHY) of which are dedicated to the studies of the Earth's atmosphere.

The GOMOS instrument consists of a star tracker used for guiding the pointing system, two spectrometers in the ultraviolet-visible–near-infrared wavelengths (UV-vis 248–690 nm, IR 750–776 nm and 916–956 nm), and two photometers, one at blue (470–520 nm) and one at red (650–700 nm) wavelengths. The photometers are used for the measurement of high vertical resolution (about 100 m) temperature profiles as well as studies of atmospheric turbulence.

The measurement principle of GOMOS, the stellar occultation technique, is presented in Figure 3.2. The spectrum of a star is first measured when the line of sight from the spacecraft to the star is above the atmosphere, and hence not affected by atmospheric absorption. While the star is in the view of the instrument, the spectrum is repeatedly recorded as the spacecraft moves along its orbit and the tangent point of the line of sight moves through the atmosphere towards the ground. Each occultation consists of attenuated stellar spectrum measurements at the altitude range from the ground to the lower thermosphere with vertical sampling resolution of 0.5–1.7 km. With the aid of the spectrum measured above the atmosphere, the measured attenuated spectra are converted to atmospheric transmissions making the measurements self-calibrated. Self-calibration removes, at least partly, the effects that the ageing of the instrument might have on the observations over longer time scales.

With the known absorption and scattering features of the different atmospheric gases the transmission spectra are inverted to density profiles of individual trace gases [*Kyrölä et al.*, 1993]. The wide spectral range from UV to near-IR enables the inversion of vertical profiles of O_3, NO_2, NO_3, H_2O, O_2 (from IR absorption), neutral density (from Rayleigh scattering) as well as aerosols. The altitude range of the profile mea-

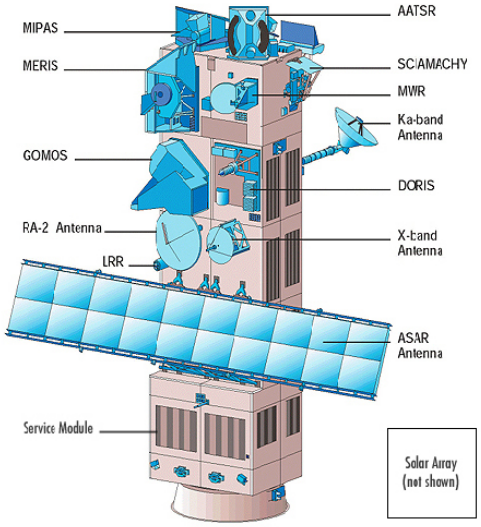

FIGURE 3.1. The Envisat satellite and the instruments on board. Figure by courtesy of the European Space Agency.

surements depends on the vertical distribution of the individual gases. For ozone the altitude range is 10–100 km but because of the low abundance of the other gases in the mesosphere and above, the altitude range of 10–50 km is recommended for them. These altitude ranges are not definite and may sometimes be extended. For example, during some periods, such as right after Solar Proton Events, when the amount of NO_2 in the mesosphere increases and exceeds normal values, the upper altitude limit rises, and NO_2 profiles can be measured even up to about 70 km altitude.

As the source of light used in the stellar occultation method is independent of the time of day and no sunlight is needed for the observations, measurements from both the day and night sides of the Earth can be attained. These are referred to as bright and dark limb measurements, respectively, the quality of the dark limb measurements being better than that of the bright limb measurements. Using several different stars as light sources and having no restriction in local time, a good global coverage, with up to 600 occultations a day, can be attained from the GOMOS observations.

As this work is focused on production and transport of NO_x during polar night conditions, GOMOS observations were particularly useful. Hence key results have been provided by GOMOS: GOMOS observations of polar nighttime ozone and NO_2 were used in PUBL. I, PUBL. II, PUBL. IV, and PUBL. V. The nighttime observations of polar NO_2 were used in PUBL. Ito quantify the increase of NO_x in the stratosphere and lower mesosphere after the Solar Proton Events of October–November 2003 and to establish the extent of the NO_x enhancements throughout the polar night. Simultaneous GOMOS ozone measurements showed long-lasting, significant ozone loss in the

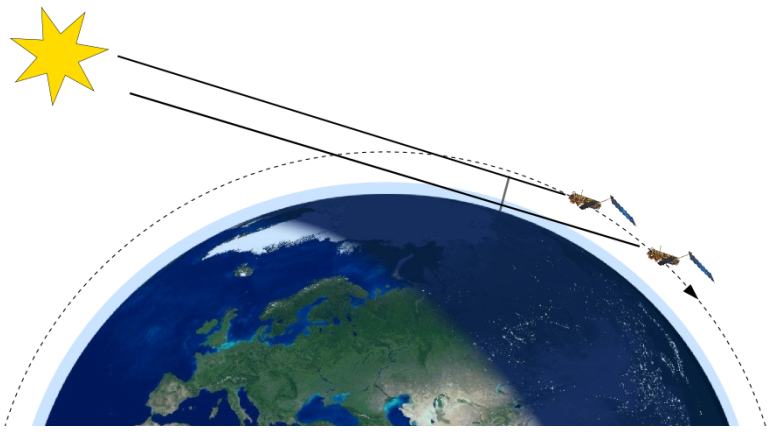

FIGURE 3.2. Stellar occultation measurement principle used by the GOMOS instrument. The dashed line illustrates the satellite orbit and the solid lines represent the lines of sight i) above the atmosphere (upper) for the reference stellar spectrum measurement and ii) through the atmosphere (lower) for the attenuated spectrum. The atmosphere is presented as a thin blue layer. Note that the figure is not to scale.

upper stratosphere. The nighttime, polar GOMOS O_3 measurements were further used to observed the disappearance of the tertiary ozone maximum during the Solar Proton Events of January 2005. In PUBL. IV the GOMOS nighttime NO_2 observations were used to establish the origin of the NO_x enhancements observed in the Northern Hemisphere in spring 2004 [*Natarajan et al.*, 2004; *Randall et al.*, 2005], and to study the latitudinal extent of the enhancements in January 2004, when they were first observed. PUBL. V utilised the available GOMOS polar nighttime NO_2 and O_3 observations from years 2002–2006.

3.2 SUBIONOSPHERIC RADIO WAVE PROPAGATION

Very Low Frequency (VLF) radio propagation, the 3–30 kHz part of the electromagnetic spectrum, is used in communication systems, for example between ground stations and submarines. The signals used in communication systems are generated by high power transmitters around the world, but VLF signals are also generated by natural processes such as lightning. As illustrated in Figure 3.3, VLF signals generated by man-made transmitters propagate in the waveguide formed by the Earth's surface and the bottom of the ionosphere (D region) located between 50 and 100 km [*Barr et al.*, 2000], thus subionospherically. Therefore all changes in the D region ionosphere lead to changes in the amplitude and phase of the received VLF signals. As a consequence of the sensitivity to changes in the D-region electron density, VLF signals may be used to monitor changes in the sources of ionisation, such as particle precipitation, in the mesosphere-lower thermosphere.

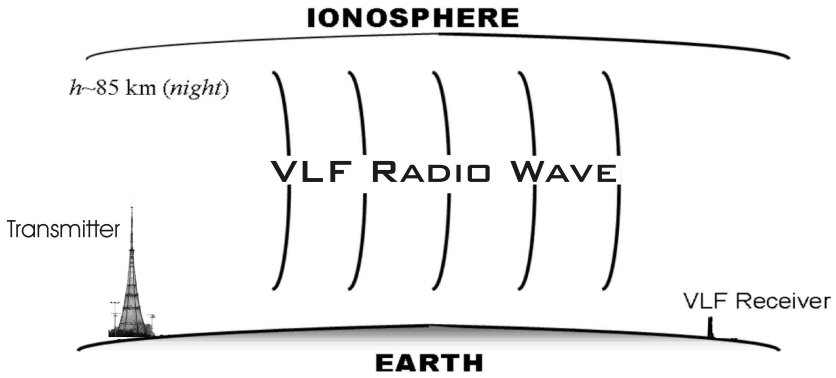

FIGURE 3.3. Schematic picture of subionospheric radio wave propagation in the waveguide formed by the Earths surface and the bottom of the ionosphere. Image courtesy of C. J. Rodger/University of Otago.

The signals coming from distant locations can be monitored by VLF receivers set up in different locations around the Earth. Figures 3.4 and 3.5 presents the locations of 15 VLF transmitters around the world and 9 VLF receivers participating in the Antarctic-Arctic Radiation-belt (Dynamic) Deposition-VLF Atmospheric Research Konsortia, AAR(D)DVARK network. As seen in Figure 3.5 several great circle paths travel across the Northern Hemisphere polar cap (L-shells $\geq$ 3) to receivers in Sodankylä, Finland and Ny Ålesund, Spitsbergen, providing a reasonably good coverage of the polar cap area.

To study signal propagation conditions, long wave propagation models such as the Long Wave Propagation Code (LWPC, *Ferguson and Snyder* [1990]) can be used. In order to calculate the signal amplitude and phase at the reception (receiver) point, information of the electron density profile parameters that define the ionospheric conditions must be provided.

VLF observations and modelling were used in PUBL. III and PUBL. IV. The electron density profile parameters for these studies were calculated using an ion and neutral chemistry model. This model, the Sodankylä Ion Chemistry model, SIC, has been used in numerous previous studies *e.g. Verronen et al.* [2002]; *Clilverd et al.* [2005]; *Enell et al.* [2005]; *Verronen et al.* [2005]; *Clilverd et al.* [2006b]; *Rodger et al.* [2006]; *Verronen et al.* [2006b] and is briefly described in section 4.2.1. As the radio wave signals are sensitive to all changes that affect the D-region ionosphere, they are also sensitive to changes in the amount of NO in mesosphere-lower thermosphere, which, when ionised by the solar or geocoronal Lyman-α, is the main source of the D-region electrons. This was utilised in PUBL. III where the radio wave observations were used to observe the descent of thermospheric NO towards the stratosphere. Figure 3.6 shows how the amplitude of a signal from Iceland (NRK) to Ny Ålesund (NYA) changes during Solar Proton Events, and an NO_x descent event (around day 100).

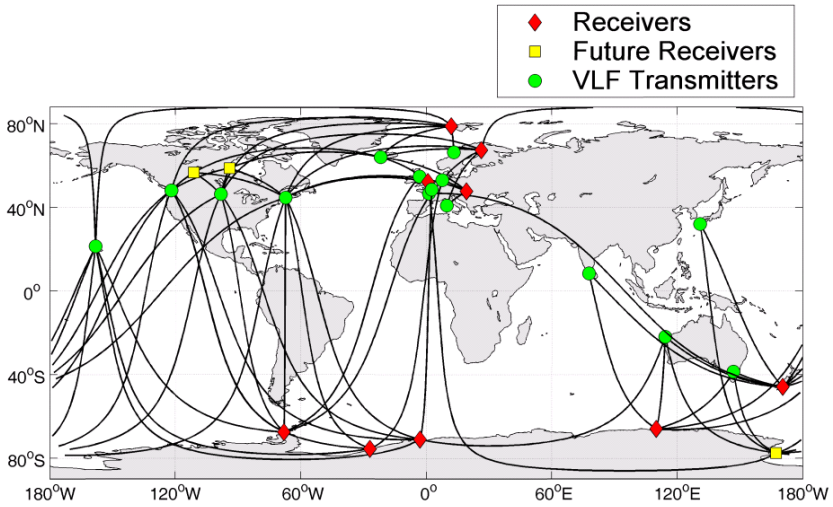

FIGURE 3.4. The global AAR(D)DVARK VLF network. Green circles mark the locations of VLF transmitters and the red diamonds the VLF receivers, yellow squares are the locations of future (as off 2006) receivers. The black lines show the great circle paths for the VLF signals. Image courtesy of C. J. Rodger/University of Otago.

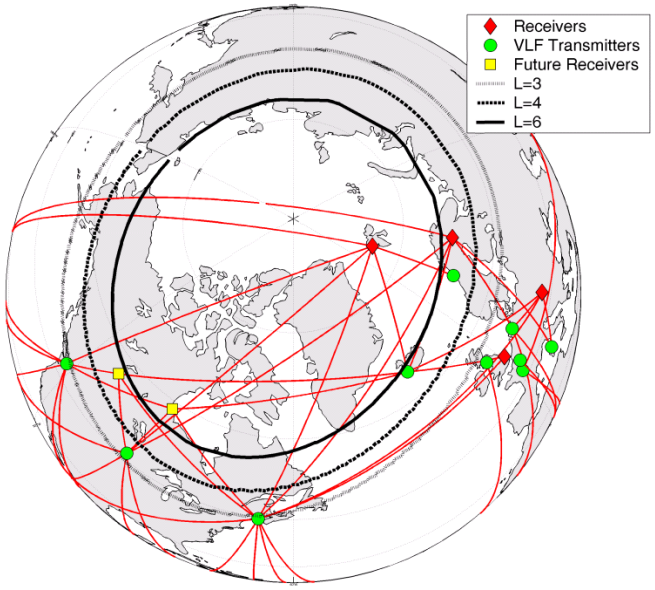

FIGURE 3.5. The Northern Hemisphere AAR(D)DVARK network. Green circles mark the locations of VLF transmitters and the red diamonds the VLF receivers, yellow squares are the locations of future (as off 2006) receivers. The red lines show the great circle paths for the VLF signals. Black circles mark the L-shells 3, 4, and 6. Image courtesy of C. J. Rodger/University of Otago.

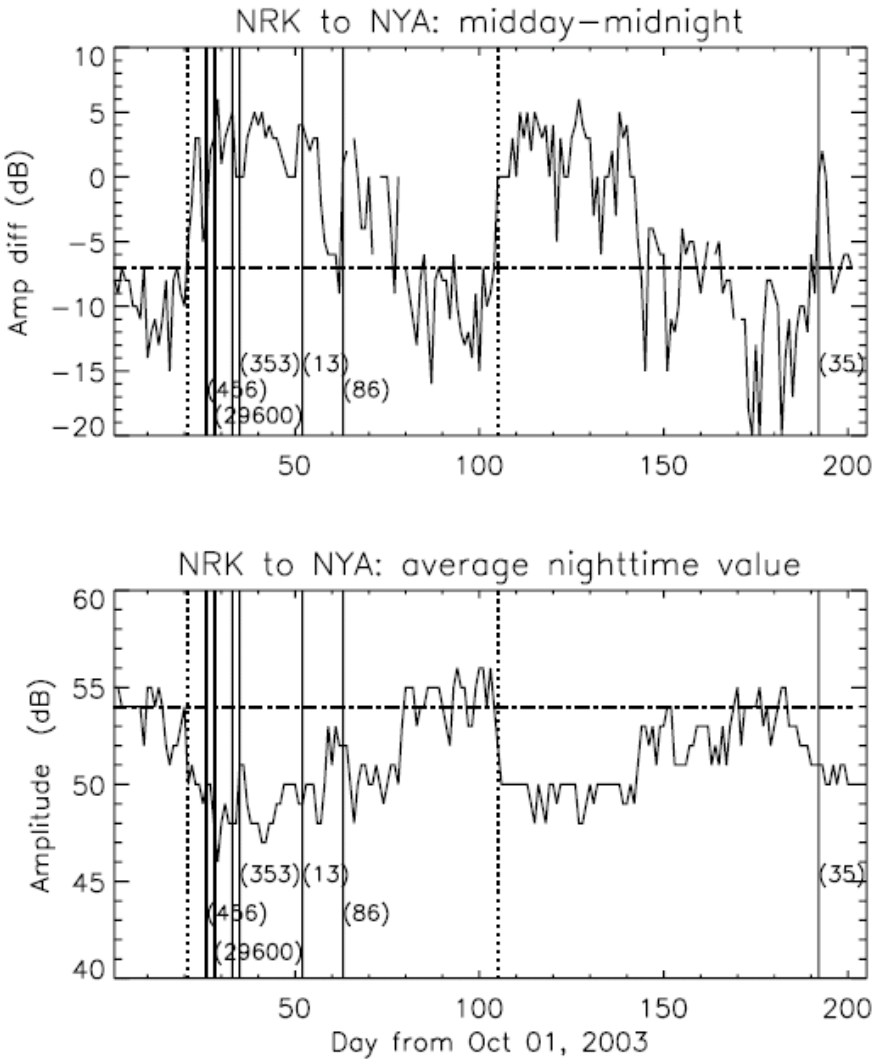

FIGURE 3.6. The winter-time differences in day-night amplitude, and average nighttime amplitude for the Iceland VLF transmitter received at Ny Ålesund. Normal values are indicated by the horizontal dash-dotted line. Times of identified solar proton events are given by solid vertical lines, while similar behaviour with no identified proton event are shown by the vertical dotted line. From PUBL. III.

4 ENERGETIC PARTICLE PRECIPITATION AND THE ATMOSPHERE

This Chapter discusses the results from PUBL. I–PUBL. V. Before the results are described, the sources of the energetic precipitating particles are briefly introduced and the coupling mechanism to the neutral atmosphere is presented.

4.1 SOURCES OF PRECIPITATING ENERGETIC PARTICLES

Figure 4.1 presents the structure of the Earth's magnetosphere. Energetic particle precipitation in the polar areas, at latitudes around 60° and higher, consists of: 1) solar energetic particles (mainly protons with energies up to hundreds of MeV) precipitating at high geomagnetic latitudes; 2) auroral precipitation in the auroral oval region originating from the plasma sheet, with electron energies up to a few tens of keV; 3) precipitating outer radiation belt particles (mainly electrons with energies up to 10 MeV, thus the outer radiation belt is also the source of relativistic electron precipitation) also forming the diffuse aurora at the equatorward portion of the auroral oval; 4) cosmic rays from outside the solar system. The most energetic of these particles are the cosmic rays with energies in the GeV energy range, but they are also fairly sparse and are not considered further here. Without measurements from space based detectors (*e.g.* particle energies and fluxes), such as those on board the GOES satellites, it is difficult to determine the origin of the particles ionising the atmosphere.

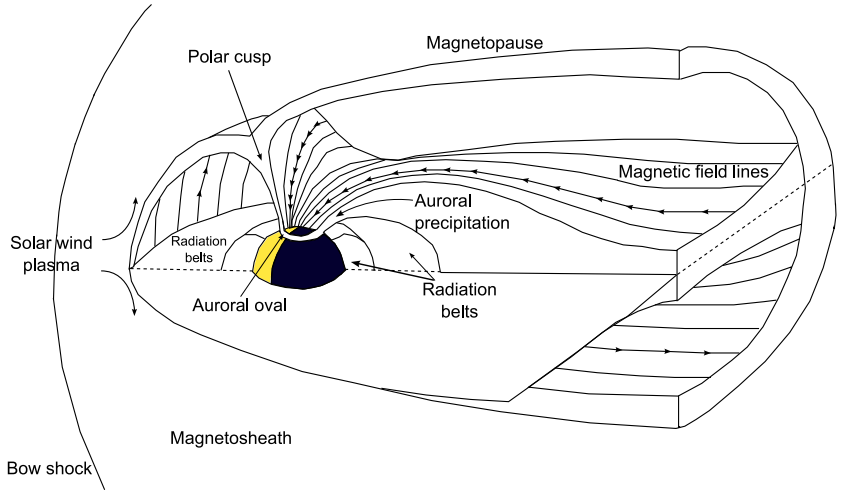

FIGURE 4.1. Structure of the Earth's magnetosphere. The yellow colour denotes the dayside of the Earth.

A Solar Proton Event (SPE), often also called Solar Particle Event, is a series of events which begins with an eruption, *i.e.* a flare or a Coronal Mass Ejection (CME),

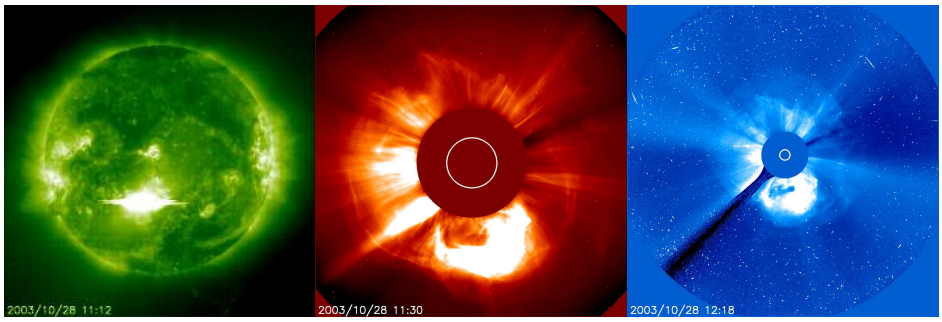

(a) EIT 195 Å (b) LASCO C2 (c) LASCO C3

FIGURE 4.2. The X17 class flare (a) and the following CME (b,c) on the 28th of October, 2003 as seen by SOHO instruments EIT (*Extreme ultraviolet Imaging Telescope*) and LASCO (*Large Angle and Spectrometric Coronagraph*). The white circle in (b,c) depicts the Sun shadowed by the coronagraph. Courtesy of SOHO/EIT and SOHO/LASCO consortiums. SOHO is a project of international cooperation between ESA and NASA.

such as those shown in Figure 4.2, in the Sun. In the eruption, charged particles, of which typically around 90 % are protons, are accelerated away from the Sun. In the acceleration, the particles may gain very high energies, up to hundreds of MeV's. Whenever these eruption are directed towards the Earth, the particles, once having reached the near-Earth space, are guided by the Earth's magnetic field. Inside the magnetosphere the particles are funnelled to the polar cap areas, near the magnetic poles (Figure 4.1) where they have access to the atmosphere [*Kivelson and Russell*, 1995]. The energy of a particle determines how deep into the atmosphere the particle can penetrate. For example, a proton which possesses 10 MeV of kinetic energy is able to ionise the atmosphere down to 65 km [*Hargreaves*, 1992]. The higher the energy the further down into the atmosphere the particle has access *e.g.* 30 MeV protons can reach 50 km altitude, 50 MeV protons can reach 40 km, and 100 MeV protons 30 km. The electrons, which have lower mass than protons, require less energy to reach the same altitudes (1 keV to reach 150 km, 10 keV to reach 108 km, and 100 keV to reach 84 km) [*Hargreaves*, 1992].

It is important to note that the motion of the precipitating charged particles is determined by the Earth's magnetic field. Since the magnetic poles are not aligned with the geographic poles, the particles do not precipitate at areas symmetrical to the geographic poles.

4.2 CHANGES IN CHEMICAL COMPOSITION

Since nitrogen and oxygen are the most predominant constituents in the neutral atmosphere, they are most affected by the ionisation. The main ions formed are N_2^+, O_2^+,

NO^+ and O^+. These ions may then further react with other ions and the neutral atoms and molecules through charge exchange reactions

$$A^+ + B \rightarrow A + B^+ \tag{4.1}$$

and recombination

$$A^+ + B^- \rightarrow \text{UNCHARGED PRODUCTS} \tag{4.2}$$

$$A^+ + e^- \rightarrow \text{UNCHARGED PRODUCTS} \tag{4.3}$$

In the initial ionisation or dissociative ionisation of the neutral atoms and molecules caused by the precipitating particles, secondary electrons may also be released

$$p^+ + A \rightarrow p^+ + A^+ + e_s^-. \tag{4.4}$$

These secondary electrons (e_s^-) have high energies and are then able to cause further ionisation.

As presented in section 2.1 the ionic reactions thus lead to production of NO_x and HO_x gases. In addition to this production, the precipitation of energetic particles have other effects on the atmosphere as well: Large SPEs have been suggested to have an influence on atmospheric temperature and dynamics [*Jackman et al.*, 2007]. The temperature changes would take place as a result of the ozone depletion or through Joule heating. Energetic electron precipitation, the subsequent NO_x enhancements and ozone loss have been suggested to have, in general, significant impacts on the polar temperatures as well as on the geopotential heights [*Rozanov et al.*, 2005]. *von Clarmann et al.* [2005] found that as a result of the enhanced HO_x, chlorine is released from the atmospheric chlorine reservoir HCl. The released chlorine is able to contribute to the ozone loss through fast reactions like

$$Cl + O_3 \rightarrow ClO + O_2, \tag{2.39}$$

and the formed ClO is able to participate in further reactions [*von Clarmann et al.*, 2005; *Brasseur and Solomon*, 2005]. Enhancements in the odd chlorine family species $ClONO_2$ have also been observed in the middle stratosphere after Solar Proton Events [*Lopéz-Puertas et al.*, 2005b].

4.2.1 Modelling EPP effects on the chemical composition

The effect that energetic particle precipitation has on the atmospheric chemical composition can be studied by using models which take into account the ionisation effects either by assuming a certain fixed amount of NO_x and HO_x produced per ion pair [*Rusch et al.*, 1981; *Jackman and McPeters*, 1985; *Jackman et al.*, 1990, 1995] or by solving the ion chemistry. The ion and neutral chemistry model SIC (Sodankylä Ion

Chemistry model) calculates the ionic and neutral reactions without the need of parameterization of the NO_x and HO_x production. The SIC model was developed as a tool to study the ionospheric D region, but since then it has been extended in both altitude and versatility, *e.g.* the current version of the model includes vertical transport, and variation of the solar flux. For each case study the solar flux is calculated using the empirical SOLAR2000 model [*Tobiska et al.*, 2000].

The earlier versions of the model were focused on the D-region ion chemistry as described by *Turunen et al.* [1996]. Later, *Verronen et al.* [2002] included neutral chemistry in the model and, afterwards, the vertical transport, including molecular and eddy diffusion [*Verronen et al.*, 2005]. As noted earlier, the production of NO_x and HO_x is not parameterized but calculated from the initial proton and electron sources. The model also takes into account the production of the ground and the first exited states of N by secondary electrons. The production is based on studies by *Rusch et al.* [1981] and depends on the total ionisation rate due to the proton and electron precipitation and galactic cosmic rays. The ionisation from galactic cosmic radiation is parameterized for solar minimum and solar maximum according to *Heaps* [1978]. The model solves vertical concentrations of 79 constituents (15 neutrals, 36 positive and 28 negative ions) in the altitude range 20–120 km with 1 km vertical step. The solar spectrum is used for wavelengths 1–423 nm. The background neutral atmosphere for the main constituents is taken from the MSISE-90 model [*Hedin*, 1991]. The model is advanced in 5 min or 15 min timesteps which allows for detailed examination of rapid chemical changes such as those connected to the HO_x species. The small timestep is also important when examining changes during sunrise and sunset [*Verronen et al.*, 2006b].

In PUBL. II the SIC model was used to examine the effects of the Solar Proton Events of January 2005 on the atmosphere. In PUBL. III and PUBL. IV the model was used to study the cause of the ionisation event observed in the radio wave measurement in the Northern Hemisphere in January 2004. It was found that instead of high energy particle precipitation, the origin of the January 2004 ionisation event was the descent of high altitude NO from the lower thermosphere to the mesosphere where it was photoionised by Lyman-α radiation.

4.3 OBSERVATIONS OF EPP EFFECTS ON THE ATMOSPHERE

In PUBL. I, PUBL. II, PUBL. IV and PUBL. V satellite observations of changes in the chemical composition of the middle atmosphere following EPP events were presented. In addition, PUBL. III and PUBL. IV utilised radio wave measurements and radio wave modelling together with an ion-neutral chemistry model in order to confirm that the large amounts of NO_x observed in the Northern Hemisphere polar cap in January - February 2004 was produced by an NO_x descent from the lower thermosphere down to the stratosphere.

4.3.1 NO_x enhancement and transport

The Solar Proton Events of October–November 2003

As discussed in section 2.2.3 the photochemical lifetime of NO_x is strongly dependent upon illumination conditions. During nighttime the chemical lifetime of the NO_x family is of the order of years throughout the middle atmosphere. Thus any increase of NO_xtaking place during the polar night may influence the middle atmosphere for several months, before the period of darkness ends.

In the beginning of the Northern Hemisphere polar winter season during 2003–2004 a series of Solar Proton Events took place. Four separate SPEs occurred within only ten days. The first of the SPEs began on October 26 from an X1-class solar flare which was immediately followed by a halo CME (see Figure 4.2). X1 refers to the intensity of the 0.1-0.8 nm X-ray flux in units of 10^{-4} Wm^{-2}. Thus an X1 flare has X-ray intensity of 1×10^{-4} Wm^{-2}. For this event the peak flux of the protons with energy greater than 10 MeV was only 466 particles s^{-1} sr^{-1} cm^{-2} (466 pfu, particle flux unit, [pfu] = flux of $>$10 MeV particles s^{-1} sr^{-1} cm^{-2}), however only two days later on October 28th another flare, this time a much more intense X17, was observed. The X17 flare was also followed by a halo CME. On October 29th the particle detectors on-board the GOES spacecraft at geosynchronous orbit measured a particle flux of 29 500 pfu. These high particle fluxes resulted in high ionisation rates in the polar atmospheres [*Jackman et al.*, 2005; *Verronen et al.*, 2005]. From the proton precipitation, the greatest forcing was placed at altitudes 30–100 km, where the ionisation maximised on October 29th. The particle forcing continued with smaller SPEs on November 2nd and 4th. Although the two last SPEs were fairly small, the November 4th event was preceded by a record setting solar flare, which was categorised X28 based on the saturation of the particle detectors on board the GOES satellites. Later, using the Earth's ionosphere as a giant X-ray detector, *Thomson et al.* [2004] suggested that the magnitude of the flare was in fact about X45. These SPE events were later named the Halloween events, as the event series began only a few days before the All Hallows day, and the particle precipitation initiated by the solar storms led to magnificent aurora observed even at mid-latitudes throughout the Halloween celebrations.

The ionisation from the proton precipitation lead to significant production of NO_x in the stratosphere-mesosphere-lower-thermosphere region. According to model results about 3.4×10^{33} NO_y molecules were produced in the aftermath of these SPEs [*Jackman et al.*, 2005], making the event the 4th largest in NO_y production since 1972 [*Jackman et al.*, 2001]. In the past, several models have predicted the SPE produced NO_x and its preservation through the dark polar winter [*Jackman et al.*, 1993; *Jackman et al.*, 1995; *Vitt and Jackman*, 1996; *Vitt et al.*, 2000]. However, no continuous measurements were available before the Halloween events. One of the instruments observing the polar atmosphere during the course of the October–November 2003 events was GOMOS. PUBL. I presents the results of the nighttime NO_2 enhancements observed at high northern latitudes. Since these are nighttime observations, the NO_2 values are

a good approximation of the total NO_x below about 60 km. The observations showed that within ten days after the events, the upper stratospheric NO_x content had risen by 400–1000 %. Two months after the beginning of the events, by the end of December 2003, the NO_x enhancements were observed to gradually descend to lower altitudes at a rate of a few tenths of km per day. A decrease in ozone was seen at stratospheric and mesospheric altitudes directly after the events. In the weeks following the SPEs, until the end of November, ozone depletion increased in the stratosphere. During December the stratospheric ozone began a gradual recovery ended by a sudden stratospheric warming at the end of December. During the stratospheric warming the polar vortex was disrupted and displaced from the pole, which advanced the mixing of air and ozone recovery. The sudden NO_x enhancement following the October–November 2003 events is shown in the top panel of Figure 4.3, which presents the polar cap (latitudes 60°N–90°N) NO_x and ozone for polar winters 2002–2003, 2003–2004, 2004–2005, 2005–2006. The gradual descent of the NO_x and the sudden stratospheric warming in December 2003 are clearly present.

NO_x produced by Energetic Particle Precipitation and vertical transport

In spring 2004, after the October–November 2003 Solar Proton Events, the highest NO_x amounts ever recorded were observed in the northern polar region [*Natarajan et al.*, 2004; *Randall et al.*, 2005; *López-Puertas et al.*, 2006]. These were first attributed to the Solar Proton Events in the previous year, but, as was suggested by *Randall et al.* [2005], it would be highly unlikely that the NO_x enhancement from the SPEs would have survived in the atmosphere without being affected by the mixing from the sudden stratospheric warming in December 2003 [*Manney et al.*, 2005] or descent during the winter. Using subionospheric Very Low Frequency radio wave propagation as discussed in section 3.2 the anomalously high NO_x was determined most likely to be of thermospheric origin (PUBL. III). A clear change in the diurnal variation of the radio wave amplitude and phase were observed on January 13, 2004, continuing for a period of over 30 days. This was consistent with the NO_x being produced by lower energy energetic particle precipitation (auroral energies) in the lower thermosphere and transported to lower altitudes rather than produced in the upper stratosphere by energetic particle precipitation such as SPEs. The thermospheric origin of the NO_x enhancements is also supported by *Funke et al.* [2007].

In PUBL. IV the subionospheric radio wave measurements were used to examine three polar winters in the northern hemisphere (2003–2004, 2004–2005, 2005–2006) with the aim of determining the periods of persistent increased mesospheric ionisation. These ionisation periods are typically caused by either intense energetic particle precipitation, such as Solar Proton Events, or by descent of thermospheric NO_x. For all winters the same radio wave propagation path was used; the signal from transmitter in Iceland (NRK) was received at Ny Ålesund. This path represents well the northern polar cap region (Figure 1 of PUBL. IV). Signatures of NO_x descent through the up-

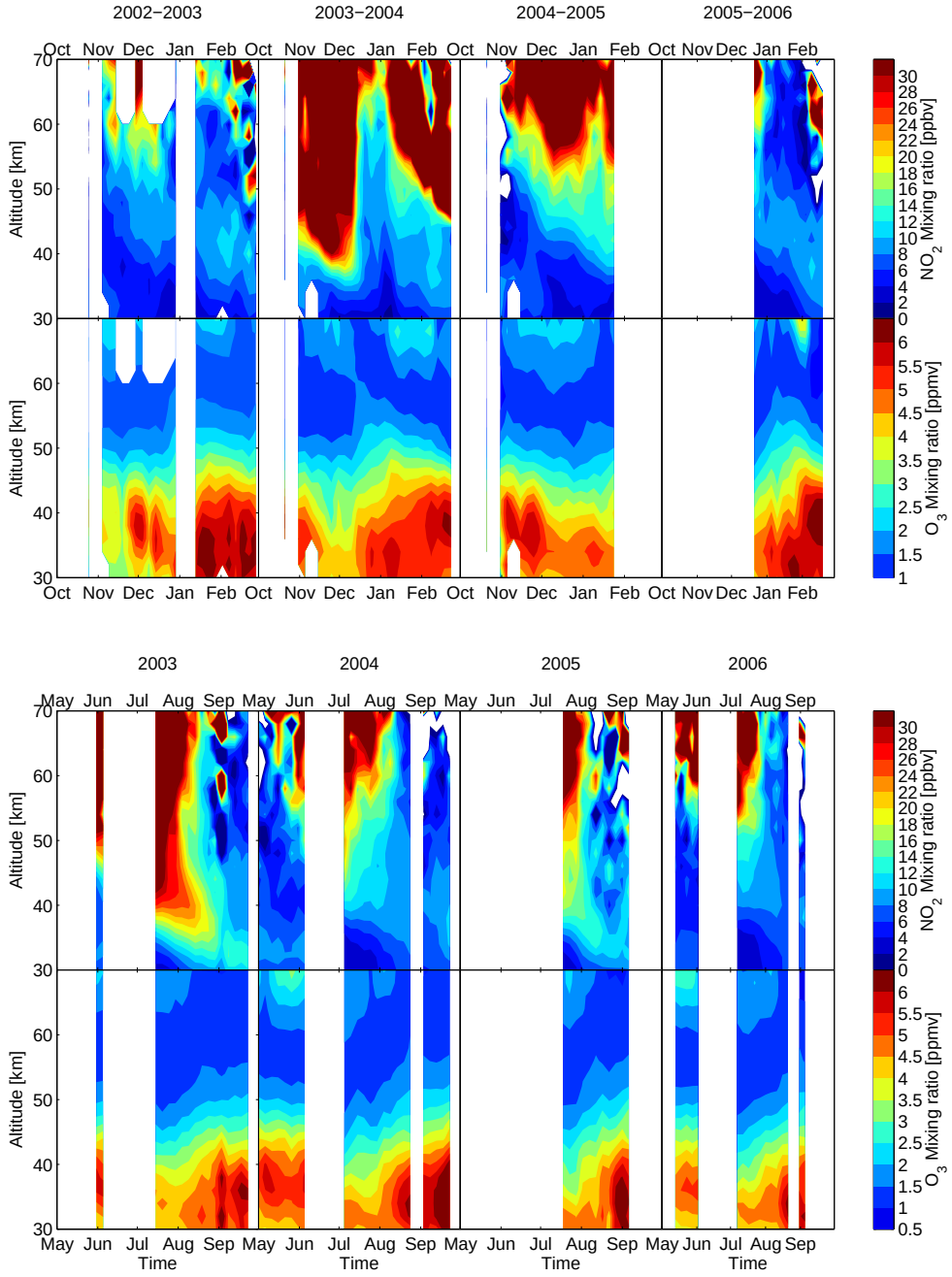

FIGURE 4.3. GOMOS nighttime NO_2 [ppbv] and ozone [ppmv] observations in the polar cap. Upper figure: Northern Hemisphere (poleward of latitude 60°N), Lower figure: Southern Hemisphere (poleward of latitude 60°S). NO_2 volume mixing ratios [ppbv = parts per billion volume] are presented in the upper rows of the panels and ozone volume mixing ratios [ppmv = parts per million volume] in the lower rows of the panels. From PUBL. V.

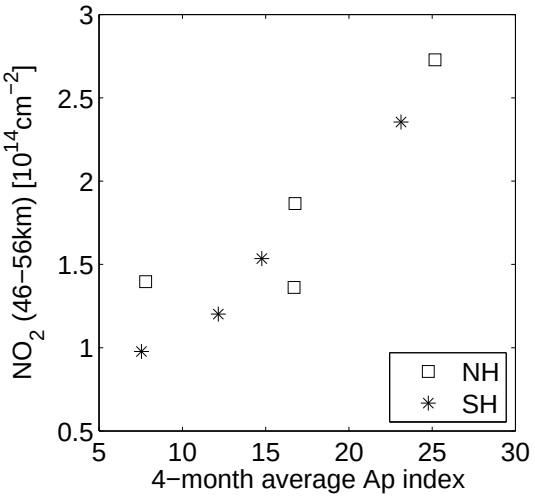

FIGURE 4.4. 4-month average A_p index and polar nighttime NO_2 column (46–56 km, poleward of latitudes $60°$N/S) from Table 1 of PUBL. V. Squares: Northern Hemisphere, Stars: Southern Hemisphere. The averaging was done for October–January in the Northern Hemisphere and May–August in the Southern Hemisphere.

per mesosphere were seen during the first winter period but not during the other two. The first of the winters was marked by two unrelated but equally important factors for significant NO_x descent: 1) there was significant ionisation from particle precipitation; 2) a strong polar vortex provided isolation of the polar air mass and strong downward transport during the winter. In the second winter only the former and in the third winter only the latter, but not both, were present. By applying NO profiles containing an enhanced NO layer to the ion and neutral chemistry model it was confirmed that the radio wave propagation measurements in January 2004 corresponded to a factor of 100 increase in mesospheric NO at altitudes 70–90 km. These results were in good agreement with observations from satellite instruments [*Randall et al.*, 2005, 2006] made at lower altitudes. By further applying different "increase" factors (*e.g.* 10, 100, 1000) and different center altitudes to the enhanced NO layer in the model NO profile, it was shown that the radio wave signal is most sensitive to an enhanced NO layer once it passes through the altitude of 80 km (Figure 6 of PUBL. IV). The model results also showed that any NO enhancement should be at least a factor of 10 larger than the normal upper mesospheric NO density in order to be observable in the radio wave.

GOMOS observations from recent polar winters (Arctic: 2002–2003, 2003–2004, 2004–2005, 2005–2006; Antarctic: 2003, 2004, 2005, 2006) show significant NO_x increases nearly every winter as seen in Figure 4.3. An average wintertime (all available observations for October–January in the Northern Hemisphere and May–August in the Southern Hemisphere) polar NO_2, partial column was calculated from these GOMOS observations around the stratopause region (46–56 km). During the polar winter months

the stratopause region works as a transit region for the NO_x descending from the lower thermosphere-mesosphere to the stratosphere (see Figure 4.3). When these values were compared with the average wintertime geomagnetic activity (geomagnetic activity index A_p averaged over the same months as the NO_2 column), a nearly linear relationship, shown in Figure 4.4, was observed. Correlation between stratospheric NO_x increases and geomagnetic activity has been observed before in the Southern Hemisphere outside the polar night area [e.g. *Siskind*, 2000; *Randall et al.*, 2007]. The GOMOS nighttime NO_2 observations show a similar correlation also in the Northern Hemisphere during the polar night period, despite the lack of stable polar vortex conditions, which are thought to be important for the Southern Hemisphere correlation. In the Northern Hemisphere NO_2 the increases in 2004–2005 are as large as expected from Antarctic correlations (PUBL. Vand Figure 4.3), although significant particle precipitation was not present.

This analysis did not include a factor describing the meteorological conditions during each winter and it should be noted that the meteorological conditions in the Northern Hemisphere are more variable than in the Southern Hemisphere. For example, exceptional meteorological conditions in the Northern Hemisphere in 2004 and 2006 [*Randall et al.*, 2007] lead to effective downward transport of thermospheric NO_x, resulting in the highest ever observed NO_x in the stratosphere in the spring and early summer. In both of these cases the stratospheric altitudes were not affected by the exceptional meteorological conditions until late January–February and thus the GOMOS October–January observations used to calculate the NO_2 columns were mainly made during more typical Northern Hemisphere dynamical conditions. Therefore the presented NO_2 columns and the found linearity between the NO_2 and average geomagnetic activity index, A_p, were not significantly affected by the exceptional meteorological conditions in 2004 and 2006, but represent the more typical Northern Hemisphere polar winter. If the Northern Hemisphere averaging period would be extended to the spring with the aid of other experiments (as GOMOS observations end in February),and included in the analysis, the linearity would, as a result of the exceptional conditions, be expected to be broken. The importance of the changing meteorological conditions are highlighted in the results from Arctic winter 2005–2006: the average NO_2 column is similar in size to year 2002–2003 and is higher than would be expected from the geomagnetic conditions. Later, in February 2006, high NO_x values around 100 ppbv were observed as a result of NO_x descent within an exceptionally strong polar vortex at the time [*Randall et al.*, 2006]

4.3.2 Mesospheric HO_x production and ozone loss

The series of Solar Protons Events beginning with an X-class solar flare on January 15, 2005, has been extensively studied under different interdisciplinary topics [*D'Andrea and Poirier*, 2005; *Clilverd et al.*, 2006a; *Kokorowski et al.*, 2006; *Simnett*, 2006; *Verro-*

nen et al., 2006a; *Moradi et al.*, 2007]. These Solar Proton Events were not exceptional in duration or flux intensity, but the fluxes of high energy particles were extraordinary large, $i.e.$ the proton energy spectrum was hard. Following the X7 class solar flare of January 20 the high energy proton fluxes (> 100 MeV) recorded at geostationary orbit by the GOES-11 satellite were equal in intensity to those recorded during the well documented October 1989 Solar Proton Events, while the lower energy fluxes remained at moderate levels. Because of this spectral hardness, the greatest impact of the precipitation occurred at altitudes lower than normal, reaching the stratosphere (see top panel of Figure 4.5).

The bottom three panels of Figure 4.5 show the results from the Sodankylä Ion and neutral Chemistry model calculations for HO_x, NO_x and ozone. The model was run for the time period January 15–24, 2005. The proton flux peaks shown in the top panel as grey dashed lines are marked in the HO_x, NO_x and ozone panels with red dashed lines. Despite the hardness of the proton spectra, the *in situ* impact on the stratospheric composition appeared to be negligible due to the rapid recovery of high energy proton fluxes to normal levels and the relatively low NO_x production at stratospheric altitudes. (PUBL. II). However, at higher altitudes in the upper mesosphere significant effects were predicted. At altitudes of about 65 km to 80 km ozone decreased up to 80 % compared with model runs with no proton precipitation. This was caused by the significant increases of the HO_x constituents. Similar ozone decreases were found from the GOMOS observations (Figure 4 of PUBL. II).

As was discussed in section 2.3, the tertiary ozone maximum occurs around 70 km altitude. In the polar mesosphere O_x is mainly in the form of ozone during nighttime. At high solar zenith angles, near the polar night terminator, photolysis of water vapour decreases due to the attenuation of solar radiation at wavelengths $<$185 nm. This reduces the amount of HO_x in the atmosphere, which in turn decreases the effect of HO_x catalytic cycles on O_x loss (see section 2.1.2), leading to a net ozone production, and the formation of the tertiary maximum. For the catalytic HO_x reactions atomic oxygen is needed. When the SPEs took place, large amount of HO_x was produced in the polar cap atmosphere. Therefore following the SPEs, in the area where the tertiary ozone maximum is observed and where the model calculations were located (70°N), the following two conditions are fulfilled: 1) the location is in the polar cap region where the energetic particles precipitate contributing to HO_x production; 2) atomic oxygen will be available for the catalytic HO_x reaction cycles through photodissociation of O_2 by radiation at wavelengths 185–242 nm in the terminator area [*Marsh et al.*, 2001]. Both are important for the efficiency of the O_x loss through HO_x catalytic reactions. This was observed as disappearance of the tertiary maximum, which had been present in both observations and modelling prior to the particle forcing from the SPEs. Once the particle forcing subsided and the HO_x production diminished, the tertiary ozone maximum re-appeared as shown in Figure 4 of PUBL. II.

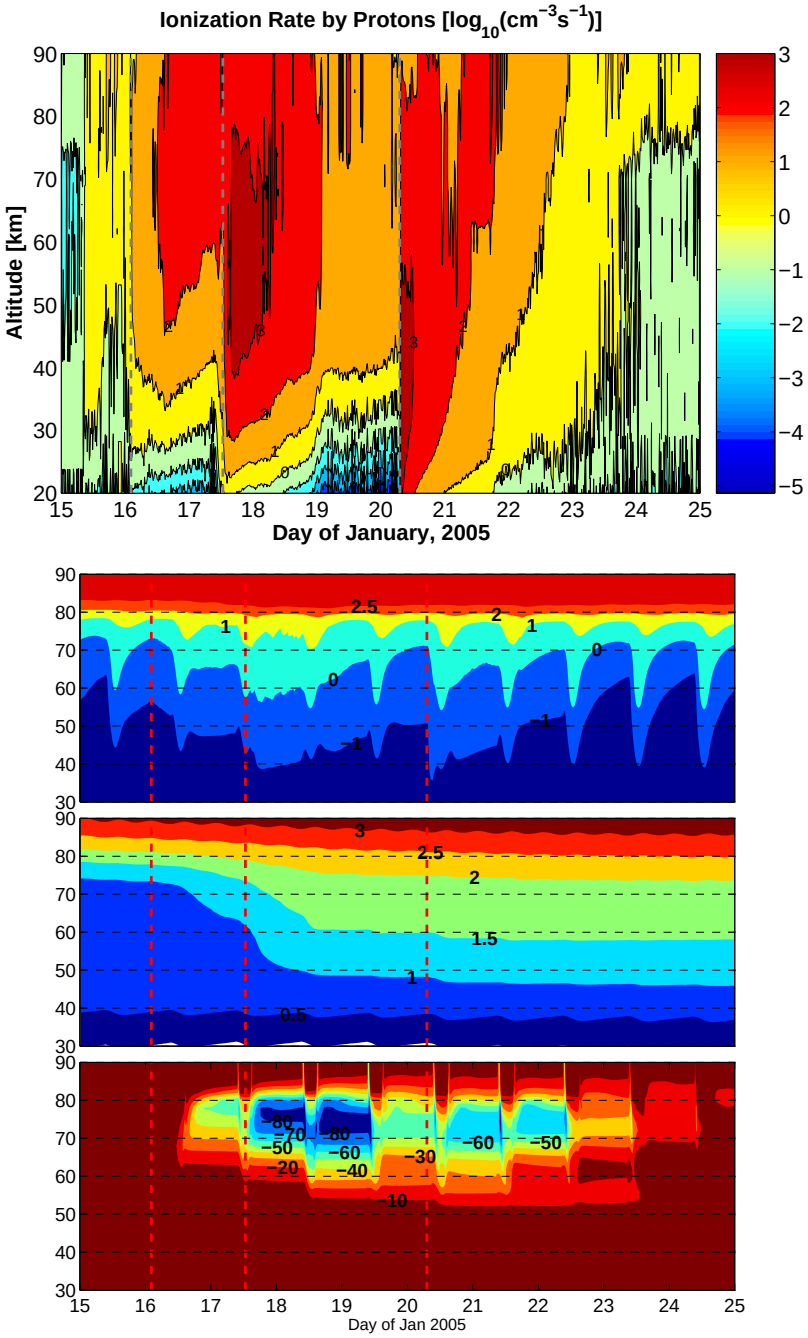

FIGURE 4.5. Top panel: Atmospheric ionisation rates from the proton precipitation, altitudes 20–90 km. The bottom 3 panels: Top: model HO_x (H + OH + HO_2) volume mixing ratio [$\log_{10}$(ppbv)], middle: model NO_x (N + NO + NO_2) volume mixing ratio [$\log_{10}$(ppbv)], bottom: O_3 change [%] due to precipitating protons. The contour lines are (0.1, $10^{-0.5}$, 1, $10^{0.5}$, 10, $10^{1.5}$, 100 ppbv), (10, 30, 50, 100, 150 ppbv), and (-80, -70, -60, -50, -40, -30, -20, -10 %) respectively. All model calculations are for location 70°N. The altitude [km] is shown in the y-axis. The dashed lines show the onsets of the Solar Proton Events. From PUBL. II.

5 SUMMARY AND CONCLUDING REMARKS

SUMMARY OF RESULTS

In PUBL. I, GOMOS observations made before, during and after the Solar Proton Events of October-November 2003 were used to study the effect of large SPEs to middle atmosphere ozone and NO_2. This was the first publication to show observations of SPE induced changes in the polar winter atmosphere, following the evolution of the changes with the progressing wintertime. The results revealed an order of magnitude increases in the upper stratospheric NO_2, lasting for several weeks after the SPEs. Consequently, ozone decreases up to 60 % from the pre-SPE values were observed in the upper stratosphere nearly a month after the events.

In PUBL. II, ozone observations from the GOMOS instrument were used with a coupled ion and neutral chemistry model to study the January 2005 Solar Proton Events effects on Northern Hemisphere polar middle atmosphere ozone. The results showed that due to the polar winter conditions, with reduced amount of sunlight, even a moderate proton flux precipitating into the atmosphere is able to disturb the odd oxygen balance through creation of odd hydrogen. This was manifested in the measurements by the disappearance of the tertiary ozone maximum during the Solar Proton Events and by a 70 % ozone depletion above 60 km. The results showed that large local perturbations in ozone may be triggered by even relatively small Solar Proton Events. Thus, it is important to take energetic particle precipitation into account in the modelling of middle atmosphere composition. The disappearance of the tertiary ozone maximum initially seen in the GOMOS observations was explained as due to the increase in the abundance of HO_x compounds at mesospheric altitudes.

A novel method to indirectly observe NO_x at upper mesospheric altitudes, 65–90 km, by the means of subionospheric radio wave propagation was developed in PUBL. III. The method is based on mesospheric NO being ionized by solar (or nighttime geocoronal) Lyman-α. This ionisation leads to changes in the electron profile, thus affecting the radio wave propagation. Subionospheric radio wave propagation measurements and modelling together with ion and neutral chemistry modelling were used to study the origin of high levels of NO_x observed at stratospheric altitudes in the polar atmosphere during the Northern Hemisphere spring 2004. The results indicated that the NO_x enhancements observed at stratospheric altitudes originated from the thermosphere above 90 km, and were not created in the mesosphere by particle precipitation. Furthermore, using radio wave observations the enhancements were already observed at high mesospheric altitudes (65–90 km) in January 2004, more than a month before reaching the stratosphere where the NO_x enhancements were observed by satellite instruments. By applying a constant, low flux particle precipitation into ion and neutral chemistry model was found that such "background" precipitation would not provide sufficient amount of NO_x to match the high values of NO_x observed later in the spring by satellite instruments. The results indicated that a factor of 100 increase in

the mesospheric NO amount would be required to explain the radio wave observations in January. By comparing this to the typical amount of NO, it was found that such an increase would be consistent with the satellite observations of enhancements NO_x later in the spring 2004.

By utilising the method of observing mesospheric NO by the means of subionospheric radio wave measurement, developed in PUBL. III, descent of high altitude NO_x during three recent Northern Hemisphere polar winters was studied in PUBL. IV. The subionospheric radio wave propagation measurements and modelling were combined with ion and neutral chemistry modelling and GOMOS polar night observations of NO_2. The radio wave observations indicated that a substantial amount of descending NO was observed in the upper mesosphere (below 90 km) only during the polar winter 2003–2004. In order to study, in detail, the effect that a layer of NO descending from above 90 km down to the stratosphere would have on the observed radio wave, the ion and neutral chemistry model was forced with an NO profile containing a 15 km-thick enhancement layer. Several model runs were executed centering the enhanced layer at different altitudes, in order to model the descent of the layer from the lower thermosphere to mesosphere. The resulting electron profiles were applied to the subionospheric radio wave propagation model and these results were then compared with the actual radio wave measurements. It was found that the observed changes in the radio wave amplitudes were well modelled by a layer of enhanced, descending NO. The model also showed that the radio wave signal is most sensitive when the descending layer of enhanced NO_x (increased by at least a factor of 10) passes through the 80 km altitude. GOMOS data were used in PUBL. IV to examine the latitudinal extent of the NO_x enhancements observed in January-February 2004 when compared with two different radio wave propagation paths. The GOMOS data showed that the descending NO_x enhancement was clearly observed at high northern latitudes, poleward of 65°N, while at lower latitudes (55°N–65°N) the signal was weaker but notably present.

In PUBL. V GOMOS measurements of NO_2 and O_3 from years 2002–2006 were used to study polar winter NO_2 enhancements and their connection to energetic particle precipitation. NO_x enhancements were found to occur in good correlation with increased high-energy particle precipitation or increased A_p index, which was used as a measure of geomagnetic activity and auroral energy particle precipitation. Furthermore, the 4-month wintertime average polar (60°N/S–90°N/S) upper-stratospheric NO_2 column was found to have a nearly linear relationship with the 4-month average wintertime A_p index. With the aid of the nighttime observations, this relationship was found on both hemispheres during the winter months.

CONCLUDING REMARKS

The GOMOS instrument has proved the power of the stellar occultation technique in observing the nighttime atmosphere. GOMOS and the two other atmospheric chemistry instruments MIPAS and SCIAMACHY on board the Envisat satellite have opened new insights to the complexity of our planet's atmosphere. In 2007 the GOMOS instrument has already lasted for over five years, and the planned lifetime of the Envisat mission has been extended to year 2010. In the coming years the scientific community will still have a strong need for new instruments capable of performing similar observations. Continuity in observations helps us to understand our planet better.

This work has not only been a success of GOMOS, but it has also shown the power of combined observations: the space-borne GOMOS observations and the ground-based radio wave observations, to achieve new insights to the Sun-Earth connection. With the improvement in the availability of atmospheric observations which now – and hopefully also in the future – routinely extend to the polar night atmosphere and to altitudes which formerly were referred to as the ignorosphere, a name formerly used to describe the D region of the ionosphere, our understanding of the complex system known as the Earth's atmosphere has increased substantially.

Recent studies of *Konopka et al.* [2007] give indications that nitrogen oxides might have an increasingly important role in the ozone balance of the polar atmospheres in the future. Their argument is based on the known assumption that in the near future the stratospheric halogen (chlorine, fluorine and bromine) levels are expected to decrease. The halogen levels have been decreasing due to the limitations in the use of the halogens after the discovery that the CFC-compounds (Chlorofluorocarbons) were the main reason of causing the stratospheric ozone hole [*Austin et al.*, 2003]. According to the case study of one recent polar winter, *Konopka et al.* found that ozone loss due to NO_x might be even twice as large as that due to the halogen compounds. These results were attained assuming that the main source of the polar winter NO_x was subtropical. Only a negligible NO_x production from particle precipitation was present. Chemistry-climate model results of *Rozanov et al.* [2005] have indicated that constant background energetic electron precipitation, which can be a significant NO_x source [*Callis et al.*, 1991; *Callis and Lambeth*, 1998] might be able to produce significant enough ozone loss (30 % in the polar areas) to induce observable changes in the polar temperature fields (ΔT of 2 K) and in the geopotential heights. The results of *Rozanov et al.* indicate that the magnitude of the atmospheric response from the energetic electron precipitation could potentially exceed the effects that arise from variation of solar UV flux. Another chemistry-climate model study [*Langematz et al.*, 2005] found that the effect of the NO_xproduced by particle precipitation, and transported into the stratosphere could alter the ozone signal of the 11-year solar cycle.

The above results already show that the effects of energetic particle precipitation on the atmosphere can be of significant importance for the Earth's atmosphere, perhaps even for the climate. Recent satellite observations have also shown that energetic par-

ticle precipitation, combined with atmospheric dynamics, is an important NO_x source in the polar winter middle atmosphere. Chemistry-climate models have systematically under-predicted NO_x in the polar winter stratosphere, probably because they do not include the downwards transport from the mesosphere. Using the latest information provided for example by the atmospheric chemistry instruments on the Envisat satellite the results on the energetic particle precipitation impact on the global climate system could be further defined. After all, whatever the effect will turn out to be, it is important for us to be aware of it even if it is *natural*, not manmade, variability.

REFERENCES

Austin, J., et al. (2003), Uncertainties and assessments of chemistry-climate models of the stratosphere, *Atmospheric Chemistry and Physics*, *3*, 1–27.

Barr, R., D. L. Jones, and C. J. Rodger (2000), ELF and VLF radio waves, *Journal of Atmospheric and Terrestrial Physics*, *62*, 1689–1718.

Bertaux, J. L., G. Megie, T. Widemann, E. Chassefiere, R. Pellinen, E. Kyrölä, S. Korpela, and P. Simon (1991), Monitoring of ozone trend by stellar occultations: The GOMOS instrument, *Advances in Space Research*, *11*(3), 237–242.

Bertaux, J. L., et al. (2004), First results on GOMOS/Envisat, *Advances in Space Research*, *33*, 1029–1035.

Brasseur, G. P., and S. Solomon (2005), *Aeronomy of the Middle Atmosphere*, 3rd revised and enlarged ed., Springer, Dordrecht.

Callaghan, P. F., and M. L. Salby (2002), Three-Dimensionality and Forcing of the Brewer-Dobson Circulation, *Journal of the Atmospheric Sciences*, *59*, 976–991.

Callis, L. B., and J. D. Lambeth (1998), NO_y formed by precipitating electron events in 1991 and 1992: Descent into the stratosphere as observed by ISAMS, *Geophysical Research Letters*, *25*, 1875–1878.

Callis, L. B., D. N. Baker, J. B. Blake, J. D. Lambeth, R. E. Boughner, M. Natarajan, R. W. Klebesadel, and D. J. Gorney (1991), Precipitating Relativistic Electrons: Their Long-Term Effect On Stratospheric Odd Nitrogen Levels, *Journal of Geophysical Research*, *96*, 2939–2976.

Callis, L. B., M. Natarajan, D. S. Evans, and J. D. Lambeth (1998), Solar atmospheric coupling by electrons (SOLACE) 1. Effects of the May 12, 1997 solar event on the middle atmosphere, *Journal of Geophysical Research*, *103*, 28,405–28,419.

Clilverd, M. A., C. J. Rodger, T. Ulich, A. Seppälä, E. Turunen, A. Botman, and N. R. Thomson (2005), Modelling a large solar proton event in the southern polar cap, *Journal of Geophysical Research*, *110*(A9), A09307, doi:10.1029/2004JA010922.

Clilverd, M. A., C. J. Rodger, and T. Ulich (2006a), The importance of atmospheric precipitation in storm-time relativistic electron flux drop outs, *Geophysical Research Letters*, *33*, L01102, doi:10.1029/2005GL024661.

Clilverd, M. A., A. Seppälä, C. J. Rodger, N. R. Thomson, P. T. Verronen, E. Turunen, T. Ulich, J. Lichtenberger, and P. Steinbach (2006b), Modelling polar ionospheric effects during the October-November 2003 solar proton events, *Radio Science*, *41*, RS2001, doi:10.1029/2005RS003290.

Crutzen, P., and S. Solomon (1980), Response of mesospheric ozone to particle precipitation, *Planetary and Space Science*, *28*, 1147–1153.

Crutzen, P. J. (1970), The influence of nitrogen oxides on the atmospheric ozone content, *Quarterly Journal of the Royal Meteorological Society*, *96*, 320–325.

Crutzen, P. J., I. S. A. Isaksen, and G. C. Reid (1975), Solar proton events: Stratospheric sources of nitric oxide, *Science*, *189*, 457–458.

D'Andrea, C., and J. Poirier (2005), Ground level muons coincident with the 20 January 2005 solar flare, *Geophysical Research Letters*, *32*, L14102, doi:10.1029/2005GL023336.

Degenstein, D. A., N. D. Lloyd, A. E. Bourassa, R. L. Gattinger, and E. J. Llewellyn (2005), Observations of mesospheric ozone depletion during the October 28, 2003 solar proton event by OSIRIS, *Geophysical Research Letters*, *32*, L03S11, doi:10.1029/2004GL021521.

Enell, C.-F., A. Kero, E. Turunen, T. Ulich, P. T. Verronen, A. Seppälä, S. Marple, F. Honary, and A. Senior (2005), Effects of D-region RF heating studied with the Sodankylä Ion Chemistry model, *Annales Geophysicæ*, *23*, 1575–1583.

Farman, J. C., B. G. Gardiner, and J. D. Shanklin (1985), Large losses of total ozone in Antarctica reveal seasonal ClO_x/NO_x interaction, *Nature*, *315*, 207–210.

Ferguson, J. A., and F. P. Snyder (1990), Computer programs for assessment of long wavelength radio communications, *Tech. Doc. 1773*, Natl. Ocean Syst. Cent., Alexandria Va.

Ferreira, S. E. S., M. S. Potgieter, R. A. Burger, B. Heber, and H. Fichtner (2001), Modulation of Jovian and galactic electrons in the heliosphere: 1. Latitudinal transport of a few MeV electrons, *Journal of Geophysical Research*, *106*, 24,979–24,988, doi:10.1029/2001JA000082.

Finlayson-Pitts, B. J., and J. N. Pitts (1999), *Chemistry of the Upper and Lower Atmosphere: Theory, Experiments, and Applications*, Academic Press.

Funke, B., M. López-Puertas, H. Fischer, G. P. Stiller, T. von Clarmann, G. Wetzel, B. Carli, and C. Belotti (2007), Comment on "Origin of the January-April 2004 increase in stratospheric NO_2 observed in northern polar latitudes" by Jean-Baptiste Renard et al., *Geophysical Research Letters*, *34*, L07813, doi:10.1029/2006GL027518.

Hargreaves, J. K. (1992), *The solar-terrestrial environment*, Cambridge Atmospheric and Space Science Series, Cambridge University Press, Cambridge, UK.

Hartogh, P., C. Jarchow, G. R. Sonnemann, and M. Grygalashvyly (2004), On the spatiotemporal behaviour of ozone within the upper mesosphere/mesopause region under nearly polar night conditions, *Journal of Geophysical Research*, *109*, D18303, doi:10.1029/2004JD004576.

Heaps, M. G. (1978), Parameterization of the cosmic ray ion-pair production rate above 18 km, *Planetary and Space Science*, *26*, 513–517.

Heath, M., A. Krueger, and P. Crutzen (1977), Solar proton event: Influence on stratospheric ozone, *Science*, *197*, 886–889.

Hedin, A. E. (1991), Extension of the MSIS Thermospheric Model into the Middle and Lower Atmosphere, *Journal of Geophysical Research*, *96*, 1159–1172.

Holton, J. R. (2004), *An Introduction to Dynamic Meteorology*, 4th ed., Elsevier Academic Press, ISBN: 0-12-354016-X.

Jackman, C. H., and R. D. McPeters (1985), The Responce of Ozone to Solar Proton Events During Solar Cycle 21: A Theoretical Interpretation, *Journal of Geophysical Research*, *90*, 7955–7966.

Jackman, C. H., and P. E. Meade (1988), Effect of Solar Proton Events in 1978 and 1979 on the Odd Nitrogen Abundance in the Middle Atmosphere, *Journal of Geophysical Research*, *93*, 7084–7090.

Jackman, C. H., A. R. Douglass, R. B. Rood, R. D. McPeters, and P. E. Meade (1990), Effect of solar proton events on the middle atmosphere during the past two solar cycles as computed using a two-dimensional model, *Journal of Geophysical Research*, *95*, 7417–7428.

Jackman, C. H., J. E. Nielsen, D. J. Allen, M. C. Cerniglia, R. D. McPeters, A. R. Douglass, and R. B. Rood (1993), The effects of the October 1989 solar proton events on the stratosphere as computed using a three-dimensional model, *Geophysical Research Letters*, *20*, 459–462.

Jackman, C. H., M. C. Cerniglia, J. E. Nielsen, D. J. Allen, J. M. Zawodny, R. D. McPeters, A. R. Douglass, J. E. Rosenfield, and R. B. Hood (1995), Two-dimensional and three-dimensional model simulations, measurements, and interpretation of the October 1989 solar proton events on the middle atmosphere, *Journal of Geophysical Research*, *100*, 11,641–11,660.

Jackman, C. H., E. L. Fleming, and F. M. Vitt (2000), Influence of extremely large solar proton events in a changing stratosphere, *Journal of Geophysical Research*, *105*, 11,659–11,670.

Jackman, C. H., R. D. McPeters, G. J. Labow, E. L. Fleming, C. J. Praderas, and J. M. Russel (2001), Northern hemisphere atmospheric effects due to the July 2000 solar proton events, *Geophysical Research Letters*, *28*, 2883–2886.

Jackman, C. H., M. T. DeLand, G. J. Labow, E. L. Fleming, D. K. Weisenstein, M. K. W. Ko, M. Sinnhuber, and J. M. Russell (2005), Neutral atmospheric influences of the solar proton events in October-November 2003, *Journal of Geophysical Research*, *110*, A09S27, doi:10.1029/2004JA010888.

Jackman, C. H., R. G. Roble, and E. L. Fleming (2007), Mesospheric dynamical changes induced by the solar proton events in October-November 2003, *Geophysical Research Letters*, *34*, L04812, doi:10.1029/2006GL028328.

Kawamoto, N., and M. Shiotani (2000), Interannual variability of the vertical descent rate in the Antarctic polar vortex, *Journal of Geophysical Research*, *105*, 11,935–11,946, doi:10.1029/2000JD900076.

Kivelson, M. G., and C. T. Russell (Eds.) (1995), *Introduction to Space Physics*, Cambridge University Press, ISBN 0-521-45714-9.

Kokorowski, M., et al. (2006), Rapid fluctuations of stratospheric electric field following a solar energetic particle event, *Geophysical Research Letters*, *33*, L20105, doi:10.1029/2006GL027718.

Konopka, P., et al. (2007), Ozone loss driven by nitrogen oxides and triggered by stratospheric warmings can outweigh the effect of halogens, *Journal of Geophysical Research*, *112*(D11), D05105, doi:10.1029/2006JD007064.

Kyrölä, E., E. Sihvola, Y. Kotivuori, M. Tikka, T. Tuomi, and H. Haario (1993), Inverse theory for occultation measurements, 1, Spectral inversion, *Journal of Geophysical Research*, *98*, 7367–7381.

Kyrölä, E., et al. (2004), GOMOS on Envisat: An overview, *Advances in Space Research*, *33*, 1020–1028.

Langematz, U., J. L. Grenfell, K. Matthes, P. M. and M. Kunze, B. Steil, and C. Brühl (2005), Chemical effects in 11-year solar cycle simulations with the Freie Universität Berlin Climate Middle Atmosphere Model with online chemistry (FUB-CMAM-CHEM), *Geophysical Research Letters*, *32*, L13803, doi:10.1029/2005GL022686.

López-Puertas, M., B. Funke, S. Gil-López, T. von Clarmann, G. P. Stiller, M. Höpfner, S. Kellmann, H. Fischer, and C. H. Jackman (2005a), Observation of NO_x enhancement and ozone depletion in the northern and southern hemispheres after the October-November 2003 solar proton events, *Journal of Geophysical Research*, *110*, A09S43, doi:10.1029/2005JA011050.

López-Puertas, M., B. Funke, T. von Clarmann, H. Fischer, and G. P. Stiller (2006), The Stratospheric and Mesospheric NO_y in the 2002-2004 Polar Winters as measured by MIPAS/ENVISAT, *Space Science Review*, *125*, 403–416, doi:10.1007/S11214-006-9073-2.

Lopéz-Puertas, M., et al. (2005b), HNO_3, N_2O_5 and $ClONO_2$ enhancements after the October-November 2003 solar proton events, *Journal of Geophysical Research*, *110*, A09S44, doi:10.1029/2005JA011051.

Manney, G. L., R. W. Zurek, A. O'Neill, and R. Swinbank (1994), On the Motion of Air through the Stratospheric Polar Vortex., *Journal of the Atmospheric Sciences*, *51*, 2973–2994.

Manney, G. L., K. Krüger, J. L. Sabutis, S. A. Sena, and S. Pawson (2005), The remarkable 2003–2004 winter and other recent warm winters in the Arctic stratosphere since the late 1990s, *Journal of Geophysical Research*, *110*(D9), D04107, doi:10.1029/2004JD005367.

Marsh, D., A. Smith, G. Brasseur, M. Kaufmann, and K. Grossmann (2001), The existence of a tertiary ozone maximum in the high latitude middle mesosphere, *Geophysical Research Letters*, *28*(24), 4531–4534.

McPeters, R., C. Jackman, and E. Stassinopoulos (1981), Observation of ozone depletion associated with Solar Proton Events, *Journal of Geophysical Research*, *86*, 12,071–12,081.

McPeters, R. D. (1986), A nitric oxide increase observed following the July 1982 solar proton event, *Geophysical Research Letters*, *13*, 667–670.

McPeters, R. D., and C. H. Jackman (1985), The response of Ozone to Solar Proton Events During Solar Cycle 21: The Observations, *Journal of Geophysical Research*, *90*, 7945–7954.

Moradi, H., A.-C. Donea, C. Lindsey, D. Besliu-Ionescu, and P. S. Cally (2007), Helioseismic analysis of the solar flare-induced sunquake of 2005 January 15, *Monthly Notices of the Royal Astronomical Society*, *374*, 1155–1163, doi:10.1111/j.1365-2966.2006.11234.x.

Natarajan, M., E. E. Remsberg, L. E. Deaver, and J. M. Russell (2004), Anomalously high levels of NO_x in the polar upper stratosphere during April, 2004: Photochemical consistency of HALOE observations, *Geophysical Research Letters*, *31*, L15113, doi:10.1029/2004GL020566.

Orsolini, Y. J., G. L. Manney, M. L. Santee, and C. E. Randall (2005), An upper stratospheric layer of enhanced HNO_3 following exceptional solar storms, *Geophysical Research Letters*, *32*, L12S01, doi:10.1029/2004GL021588.

Randall, C. E., V. L. Harvey, C. S. Singleton, P. F. Bernath, C. D. Boone, and J. U. Kozyra (2006), Enhanced NO_x in 2006 linked to upper stratospheric Arctic vortex, *Geophysical Research Letters*, *33*, L18811, doi:10.1029/2006GL027160.

Randall, C. E., et al. (2005), Stratospheric effects of energetic particle precipitation in 2003-2004, *Geophysical Research Letters*, *32*, L05802, doi:10.1029/2004GL022003.

Randall, C. E., et al. (2007), Energetic particle precipitation effects on the Southern Hemisphere stratosphere in 1992–2005, *Journal of Geophysical Research*, *112*, D08308, doi:10.1029/2006JD007696.

Reid, G. C., S. Solomon, and R. R. Garcia (1991), Response of the middle atmosphere to the solar proton events of August-December, 1989, *Geophysical Research Letters*, *18*, 1019–1022.

Rodger, C. J., M. A. Clilverd, P. T. Verronen, T. Ulich, M. J. Jarvis, and E. Turunen (2006), Dynamic geomagnetic rigidity cutoff variations during a solar proton event, *Journal of Geophysical Research*, *111*, A04222, doi:10.1029/2005JA011395.

Rohen, G., et al. (2005), Ozone depletion during the solar proton events of October/November 2003 as seen by SCIAMACHY, *Journal of Geophysical Research*, *110*, A09S39.

Rosenfield, J. E., and M. R. Schoeberl (2001), On the origin of polar vortex air, *Journal of Geophysical Research*, *106*, 33,485–33,498, doi:10.1029/2001JD000365.

Rosenfield, J. E., P. A. Newman, and M. R. Schoeberl (1994), Computations of diabatic descent in the stratospheric polar vortex, *Journal of Geophysical Research*, *99*, 16,677.

Rozanov, E., L. Callis, M. Schlesinger, F. Yang, N. Andronova, and V. Zubov (2005), Atmospheric response to NO_y source due to energetic electron precipitation, *Geophysical Research Letters*, *32*, L14811, doi:10.1029/2005GL023041.

Rusch, D. W., and C. A. Barth (1975), Satellite measurements of nitric oxide in the polar region, *Journal of Geophysical Research*, *80*, 3719–3721.

Rusch, D. W., J.-C. Gérard, S. Solomon, P. J. Crutzen, and G. C. Reid (1981), The effect of particle precipitation events on the neutral and ion chemistry of the middle atmosphere – I. Odd nitrogen, *Planetary and Space Science*, *29*, 767–774.

Salby, M. L., and P. F. Callaghan (2006), Residual mean transport in the stratosphere: Contributions from wave driving and seasonal transience, *Journal of Geophysical Research*, *111*(D10), D22304, doi:10.1029/2005JD006767.

Seinfeld, J. H., and S. N. Pandis (1998), *Atmospheric chemistry and physics: from air pollution to climate change*, A Wiley-Interscience Publication, Wiley, New York, ISBN: 0471178152.

Semeniuk, K., J. C. McConnell, and C. H. Jackman (2005), Simulation of the October-November 2003 solar proton events in the CMAM GCM: Comparison with observations, *Geophysical Research Letters*, *32*, L15S02, doi:10.1029/2005GL022392.

Shimazaki, T. (1984), *Minor Constituents in the Middle Atmosphere (Developments in Earth and Planetary Physics, No 6)*, D. Reidel Publishing Co., Dordrecht, Holland.

Simnett, G. M. (2006), The timing of relativistic proton acceleration in the 20 January 2005 flare, *Astronomy and Astrophysics*, *445*, 715–724, doi:10.1051/0004-6361:20053503.

Siskind, D. E. (2000), On the coupling between the middle and upper atmospheric odd nitrogen, in *Atmospheric science across the stratopause*, *Geophysical Monograph*, vol. 123, pp. 101–116, American Geophysical Union.

Siskind, D. E., L. Coy, and P. Espy (2005), Observations of stratospheric warmings and mesospheric coolings by the TIMED SABER instrument, *Geophysical Research Letters*, *32*, L09804, doi:10.1029/2005GL022399.

Solomon, S. (1999), Stratospheric ozone depletion: a review of concepts and history, *Reviews of Geophysics*, *37*(3), 275–316.

Solomon, S., D. W. Rusch, J.-C. Gérard, G. C. Reid, and P. J. Crutzen (1981), The effect of particle precipitation events on the neutral and ion chemistry of the middle atmosphere: II. Odd hydrogen, *Planetary and Space Science*, *8*, 885–893.

Solomon, S., P. J. Cruzen, and R. G. Roble (1982), Photochemical coupling between the thermosphere and the lower atmosphere 1. Odd nitrogen from 50 to 120 km, *Journal of Geophysical Research*, *87*(C9), 7206–7220.

Solomon, S., G. C. Reid, D. W. Rusch, and R. J. Thomas (1983), Mesospheric ozone depletion during the solar proton event of July 13, 1982 Part II. Comparisons between theory and measurements, *Geophysical Research Letters*, *10*, 257–260.

Sprigg, W. A. (Ed.) (2000), *Nasa Workshop in Sun-Climate Connections: Summary Report*, University of Arizona, Tucson, USA.

Thomson, N. R., C. J. Rodger, and R. L. Dowden (2004), Ionosphere gives size of greatest solar flare, *Geophysical Research Letters*, *31*, L06803, doi:10.1029/2003GL019345.

Tobiska, W. K., T. Woods, F. Eparvier, R. Viereck, L. D. B. Floyd, G. Rottman, and O. R. White (2000), The SOLAR2000 empirical solar irradiance model and forecast tool, *Journal of Atmospheric and Terrestrial Physics*, *62*, 1233–1250.

Turunen, E., H. Matveinen, J. Tolvanen, and H. Ranta (1996), D-region ion chemistry model, in *STEP Handbook of Ionospheric Models*, edited by R. W. Schunk, pp. 1–25, SCOSTEP Secretariat, Boulder, Colorado, USA.

Verronen, P. T., E. Turunen, T. Ulich, and E. Kyrölä (2002), Modelling the effects of the October 1989 solar proton event on mesospheric odd nitrogen using a detailed ion and neutral chemistry model, *Annales Geophysicæ*, *20*, 1967–1976.

Verronen, P. T., A. Seppälä, M. A. Clilverd, C. J. Rodger, E. Kyrölä, C.-F. Enell, T. Ulich, and E. Turunen (2005), Diurnal variation of ozone depletion during the October-November 2003 solar proton events, *Journal of Geophysical Research*, *110*, A09S32, doi:10.1029/2004JA010932.

Verronen, P. T., A. Seppälä, E. Kyrölä, J. Tamminen, H. M. Pickett, and E. Turunen (2006a), Production of odd hydrogen in the mesosphere during the January 2005 solar proton event, *Geophysical Research Letters*, *33*, L24811, doi: 10.1029/2006GL028115.

Verronen, P. T., T. Ulich, E. Turunen, and C. J. Rodger (2006b), Sunset transition of negative charge in the D-region ionosphere during high-ionization conditions, *Annales Geophysicæ*, *24*, 187–202.

Vitt, F. M., and C. H. Jackman (1996), A comparison of sources of odd nitrogen production from 1974 through 1993 in the Earth's middle atmosphere as calculated using a two-dimensional model, *Journal of Geophysical Research*, *101*, 6729–6740, doi: 10.1029/95JD03386.

Vitt, F. M., T. P. Armstrong, T. E. Cravens, G. A. M. Dreschhoff, C. H. Jackman, and C. M. Laird (2000), Computed contributions to odd nitrogen concentrations in the Earth's polar middle atmosphere by energetic charged particles, *Journal of Atmospheric and Terrestrial Physics*, *62*, 669–683.

von Clarmann, T., et al. (2005), Experimental evidence of perturbed odd hydrogen and chlorine chemistry after the October 2003 solar proton events, *Journal of Geophysical Research*, *110*, A09S45, doi:10.1029/2005JA011053.

Weeks, L. H., R. S. Cuikay, and J. R. Corbin (1972), Ozone Measurements in the Mesosphere During The Solar Proton Event of 2 November 1969, *Journal of the Atmospheric Sciences*, *29*, 1138–1142.